9. Natural Time Analysis of Electrocardiograms

Abstract. Here, we present the results obtained from the natural time analysis of electrocardiograms. Considering that a general agreement about whether normal heart dynamics are chaotic or not is still lacking, and that a physiological time series may be due to a mixed process, stochastic and deterministic, we use here the concept of entropy which is equally applicable to deterministic as well as stochastic processes. Sudden cardiac death is a frequent cause of death and may occur even if the electrocardiogram seems to be strikingly similar to that of a healthy individual. Upon employing, however, the fluctuations of the entropy in natural time, when a time window of certain length is sliding each time by one "pulse" (heartbeat) through the whole time series, sudden cardiac death individuals (SD) can be clearly distinguished from the truly healthy individuals. Furthermore, by using the complexity measures introduced in § 3.6.1 to quantify the change of the natural entropy fluctuations either by changing the time window length scale or by shuffling the "pulses" randomly, we can achieve the classification of individuals into three categories: healthy, heart disease patients and SD. In addition, when considering the entropy change under time reversal, at certain time window length scales (which have a clear physical meaning), not only can the SD risk be identified, but also an estimate of the time of the impending cardiac arrest can be provided. In particular, after the maximization of the amplitude of ΔS at the scale of 13 heartbeats, ventricular fibrillation starts within $\approx$3 hours in 16 out of 18 SD. Finally, an $1/f$ model is proposed in natural time which leads to results that are consistent with the progressive modification of heart rate variability in healthy children and adolescents. The model results in complexity measures that separate healthy dynamics from heart disease patients as well as from SD.

9.1 Natural time analysis of the RR, QRS and QT time series

9.1.1 Introduction

The advantages of using the concept of the entropy in the analysis of a physiological time series in general, and of electrocardiograms (ECG) in particular, has been already

P.A. Varotsos et al., *Natural Time Analysis: The New View of Time: Precursory Seismic Electric Signals, Earthquakes and other Complex Time Series*, Springer Praxis Books, DOI 10.1007/978-3-642-16449-1_9,

explained in Section 3.1. In addition, it was explained there why the complexity measures associated with the entropy S defined in natural time (which is a *dynamic* entropy) have certain advantages compared to those based on *static* entropy (e.g. Shannon entropy). Earlier attempts in the ECG analysis have actually used measures related to dynamic entropy. For example, the so-called approximate entropy (AE) [48] or sample entropy (SE) [51] have been used earlier by other authors. Examples showing that the procedure developed here gives [63] better results than that based on AE or SE will be put forward later in § 9.2.3. Also, Costa et al. [11] introduced the multiscale entropy approach, the algorithm of which is based on AE or SE, calculating the entropy at different scales. As for the S, it differs essentially from the other entropies, because it is defined [61, 62] in an entirely different time-domain (see Fig. 9.1(b)). Moreover, as already mentioned (§ 4.8.3), in order to discriminate *similar-looking* electric signals emitted from systems of different dynamics, the following seems to hold [68]:

> Signals that have S values more or less comparable to S_u (*which is the case of all ECG*, see Fig. 9.11 that will be discussed later) can be better classified by the complexity measures relevant to the fluctuations δS of the entropy.

If the S values differ *markedly* from S_u (which is usually the case for SES and AN), the classification of these signals should be preferably made by the use of the S values themselves (see Section 4.10). Hereafter, we focus on the case of ECG.

In a single sinus (normal) cycle of an ECG, the turning points are traditionally labeled with the letters Q, R, S, T; see Fig. 9.1(a). It has been clinically observed that the QT interval usually exhibits prolonged values before cardiac death (see Ref. [26] and references therein). In Fig. 9.1(b) we show how the QT interval time series can be read in natural time. By the same token, one can read in natural time the RR (beat-to-beat) interval time series (see Figs. 2.2(a) and 2.2(b)) as well as the QRS interval time series. The RR and

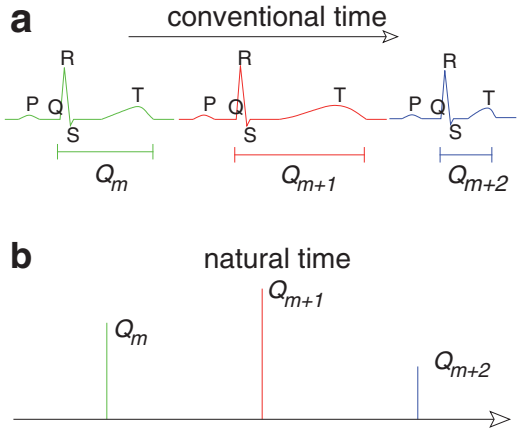

Fig. 9.1 (a) Schematic diagram (not in scale) of a three heartbeat excerpt of an ECG in the usual (conventional) time domain. Only the durations Q_m,Q_{m+1},Q_{m+2} of the QT interval (marked in each single cycle of the ECG corresponding to one heartbeat) are shown. (b) The QT interval time series of (a) read in natural time; the vertical bars are *equally* spaced and the length of each bar denotes the duration of the corresponding QT interval marked in (a). Taken from Ref. [66].

QRS intervals (mainly the RR) can be automatically detected [32, 30, 31, 22] more easily than the QT.

Sudden cardiac death, which is the primary cause of mortality in the industrialized world [7], may occur even if the ECG looks to be similar to that of truly healthy (H) humans.

Here, we present a surrogate data analysis which differentiates the ECG of H from those of sudden cardiac death individuals (SD) based on the fluctuations of the entropy S in natural time.

The fact that a system contains nonlinear components does not necessarily reflect that a specific signal we measure from the system also exhibits nonlinear features. Thus, before analyzing this signal by applying nonlinear techniques, we must first clarify if the use of such techniques is justified by the data available. The method of surrogate data has been extensively used to serve such a purpose (see Ref. [55] for a review). Surrogate data refer to data that preserve certain linear statistic properties of the experimental data, but are *random* otherwise [8, 57]. These data are prepared by various procedures, e.g., see Ref. [57]. Here, the surrogate data are obtained by shuffling the Q_k randomly and hence their distribution is conserved. Applying such a procedure, we do the following: consider the null hypothesis that the data consist of *independent* draws from a fixed probability distribution of the dwell times; if we find significantly different serial correlations in the data and their shuffles, we can reject the hypothesis of *independence* [55]. In other words, the tested null hypothesis is that Q_k are independent and identically distributed (i.i.d.) random variables, i.e., that there are no correlations between the lengths of consecutive intervals. If the original (continuous) time series is Markovian then the null hypothesis for the Q_k should hold, i.e., the Q_k are i.i.d. random variables. The terminology "Markovian" here always refers to the original time series.

Following § 3.6.1, as a measure of the natural time entropy S fluctuations we consider the standard deviation δS when we calculate the value of S for a number of consecutive pulses and study how S varies when sweeping this time-window through the whole time series. In all examples, we use here a sliding window of length 3 to 10 pulses, except otherwise stated. Concerning the symbols: we reserve δS *only* for the case when the calculation is made by a *single* time-window, e.g., 5 pulses. The symbol $\overline{\delta S}$ denotes the average of the δS values calculated for a sequence of single time-windows, e.g., 3, 4 and 5 pulses. Finally, $\langle \delta S \rangle$ stands for the δS values averaged over a group of individuals, e.g., the healthy subjects. The subscript "*shuf*" means that the relevant quantity refers to data obtained by shuffling Q_k randomly.

We used here the QT database from physiobank [14] (see also Ref. [31]), which is publicly accessible and consists of 105 fifteen-minute excerpts of Holter recordings as follows: 10 from MIT-BIH Normal Sinus Rhythm Database (i.e., healthy subjects, hereafter labeled H), 15 from MIT-BIH Arrhythmia Database (MIT), 13 from MIT-BIH Supraventricular Arrhythmia Database (MSV), 6 from MIT-BIH ST Change Database (MST), 33

from the European ST-T Database (EST), 4 from MIT-BIH Long-Term ECG Database (LT) and 24 from sudden cardiac death patients from BIH(SD) (BIH denotes the Beth Israel Hospital).

9.1.2 The quantities δS and δS_{shuf}. The non-Markovianity of electrocardiograms

We now investigate if the δS values alone can "recognize" the non-Markovianity in ECG [67]. In Fig. 9.2, we plot, for the QRS interval time series, the δS value averaged over each of the aforementioned seven groups versus the time-window length. Since all time series of these seven groups have $\approx 10^3$ intervals, we insert in the same figure the results calculated for a Markovian case of comparable length $\approx 10^3$. In particular, we consider a *dichotomous* Markovian time series, in which we recall (e.g. § 4.1.1 and § 4.1.3) that the dwell times (Q_k) are exponentially distributed. (Since in the calculation of S only ratios of Q_k are involved the result does not depend on the transition rates of the Markovian process.) An inspection of this figure shows that the Markovian case exhibits δS values that are roughly one order of magnitude larger than those of the seven groups of ECG, which clearly points to the non-Markovianity of *all* the signals in these groups. We emphasize that the same conclusions are drawn if we consider, instead of QRS, the time series of QT, or RR intervals.

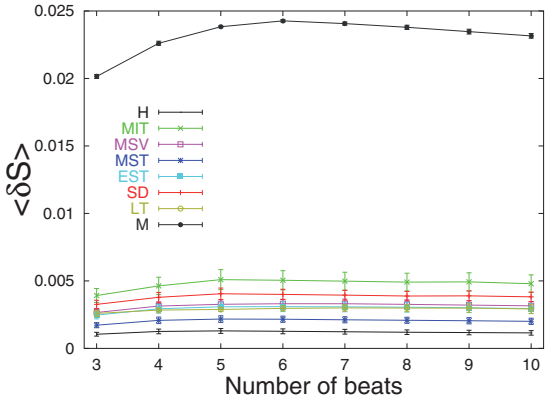

Fig. 9.2 The $\langle \delta S \rangle$ values for the QRS intervals (see the text) of the seven groups of ECG versus the time-window length. The corresponding values for a Markovian time series (10^3 pulses, labeled M) are also plotted. Taken from Ref. [67].

In summary, the δS value alone can recognize the non-Markovianity in ECG.

We now study δS_{shuf} (§ 3.6.1). Having in mind Eq. (3.63), in Fig. 9.3(a) we plot, for each of the 105 individuals, the value of σ/μ versus the corresponding value of $\overline{\delta S_{shuf}}$ (time-window range 3–10 beats) for the RR intervals. The same is repeated in Figs. 9.3(b) and 9.3(c) for the QT and QRS intervals, respectively. All these three plots, can be described by linear behavior and a least-squares fitting to a straight line passing through the origin leads to the following slopes: 38.6 ± 0.6, 36.8 ± 0.2 and 40.1 ± 0.4, for the RR, QT and QRS intervals, respectively. This points to the conclusion that δS_{shuf} provides a

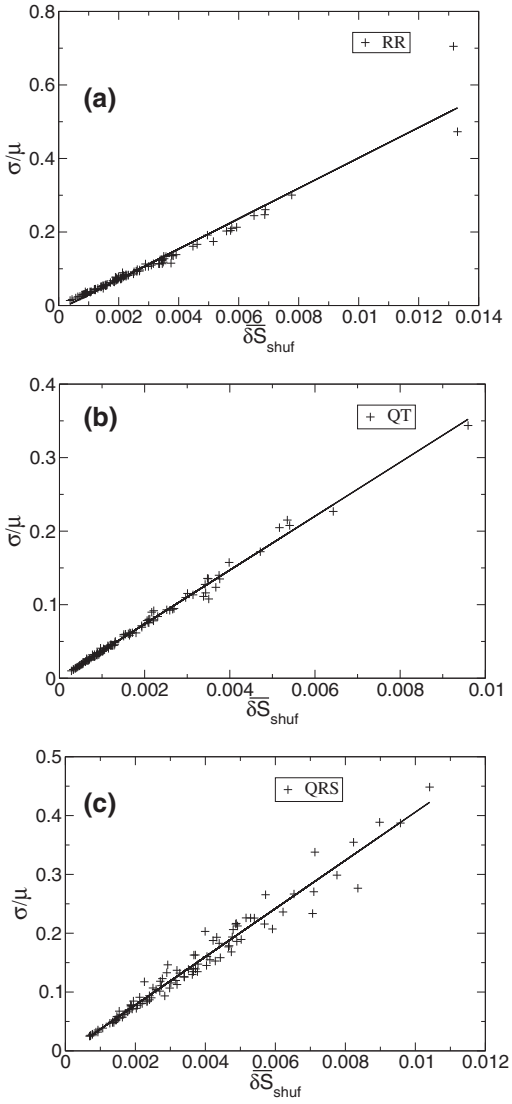

Fig. 9.3 The σ/μ value, for each of the 105 individuals, versus the corresponding $\overline{\delta S_{shuf}}$ value for the (a) RR, (b) QT and (c) QRS intervals. The identity of the individual associated with each point can be found in Ref. [64]. Taken from Ref. [67].

measure of σ/μ. Note that, although these three slopes are more or less comparable, they differ by amounts lying outside their standard error. Furthermore, if we study *altogether* the RR, QT and QRS intervals, for the 10 healthy humans *only* (Fig. 9.4), a good linearity of σ/μ versus $\overline{\delta S_{shuf}}$ results with a slope 37.5 ± 0.4. (note that if we study each of the three intervals separately, we find slopes that agree within the error margins, i.e., 37.5 ± 0.4, 37.1 ± 0.7 and 37.8 ± 0.1 for the RR, QT and QRS intervals, respectively). The origin of this *common* behavior in the *healthy* humans merits further investigation.

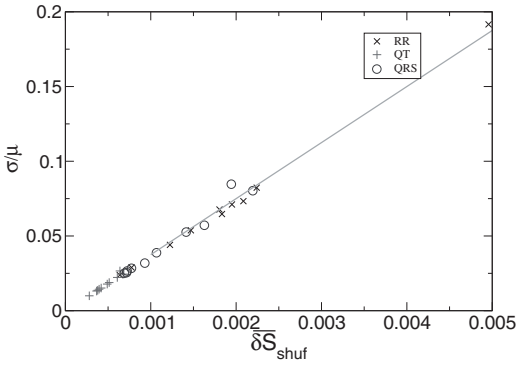

Fig. 9.4 The σ/μ value for RR, QT and QRS intervals of the ten H versus the corresponding $\overline{\delta S_{shuf}}$ value (time-window range 3–10 beats). The straight line results from a least-squares fit of all the thirty points. For the identity of the individual associated with each point see Ref. [64]. Taken from Ref. [67].

One could argue that Q_k may become i.i.d. upon their shuffling. In § 3.4.6, we showed that, when Q_k are i.i.d., δS is actually proportional to σ/μ, since the following relation holds (see Eq. (3.63)):

$$\delta S_{shuf} = \frac{\sigma}{\mu}\frac{1}{\sqrt{N-1}}\sqrt{\sum_{k=1}^{N}\left(\frac{k}{N}\ln\frac{k}{eN\overline{\chi}}\right)^2\frac{1}{N} - \left(\sum_{k=1}^{N}\frac{k}{N^2}\ln\frac{k}{eN\overline{\chi}}\right)^2} \tag{9.1}$$

where

$$\overline{\chi} = \sum_{k=1}^{N}\frac{k}{N^2} = \frac{1}{2} + \frac{1}{2N} \tag{9.2}$$

and e denotes, as usually, the base of the natural logarithms. The relation (9.1) reveals that δS_{shuf} versus σ/μ must be a straight line with a slope ranging from 34.2 to 40.4, for a time-window length 3 to 10. This result is comparable with the slopes determined above from the analysis of the ECG data.

We now proceed to compare δS_{shuf} with δS in ECG. We first point out that for a Markovian case we expect $\overline{\delta S_{shuf}} = \overline{\delta S}$ in view of the following:

Since, by definition, δS_{shuf} corresponds to the entropy fluctuations upon shuffling Q_k *randomly*, it is naturally expected that in a *Markovian* case the two quantities δS and δS_{shuf} *should* coincide. Note, however, that the reverse is *not* always true. The equality $\overline{\delta S_{shuf}} = \overline{\delta S}$ may also hold for *non*-Markovian time series, as will be demonstrated below with precise examples.

Figure 9.5(a) depicts the $\overline{\delta S}$ values, calculated for each of the 105 individuals, versus the corresponding $\overline{\delta S_{shuf}}$ for the RR intervals (time-window range 3–10 beats). The same is repeated in Figs. 9.5(b) and 9.5(c) for the QT and QRS intervals, respectively. In each case, we also plot the straight line $\overline{\delta S_{shuf}} = \overline{\delta S}$ to visualize that the vast majority of points fall below this line. The non-equality of $\overline{\delta S_{shuf}}$ and $\overline{\delta S}$ has been also verified by applying the Wilcoxon paired signed-rank test, which is recommended [42] to be fol-

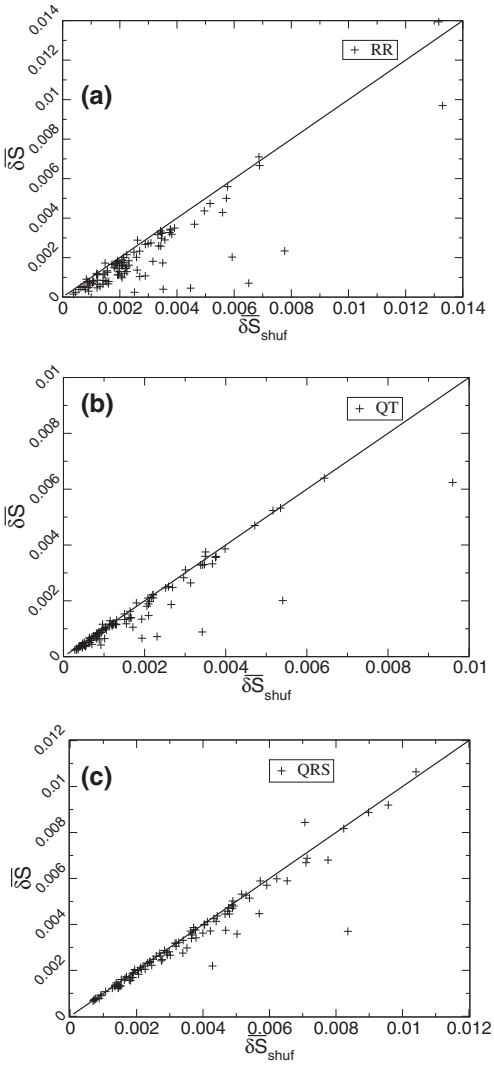

Fig. 9.5 The $\overline{\delta S}$ value, for each of the 105 individuals versus the corresponding $\overline{\delta S}_{shuf}$ value for (a) RR, (b) QT and (c) QRS intervals. The straight line, drawn in each case, corresponds to $\overline{\delta S}_{shuf} = \overline{\delta S}$. For the identity of the individual associated with each point see Ref. [64]. Taken from Ref. [67].

lowed for non-Gaussian paired data. The tested null hypothesis is that the means of $\overline{\delta S}_{shuf}$ and $\overline{\delta S}$ are the same and is rejected at a level of significance well below 0.01, since the data of Figs. 9.5(a),(b) and (c) lead to normally distributed variables $z = -8.29$, -6.81 and -6.32, respectively (note that the corresponding one-tailed asymptotic significance is given by $P(Z < z)$, i.e., the probability of obtaining a normally distributed variable obeying $N(0,1)$ that is smaller than z). Note that a least-squares fit to a straight line passing through the origin, results in the following expressions: $\delta S = 0.76(3)\delta S_{shuf}$, $\delta S = 0.85(2)\delta S_{shuf}$, $\delta S = 0.94(2)\delta S_{shuf}$ for the Figs. 9.5(a), 9.5(b), 9.5(c), respectively. The sampling rate f_{exp} in ECG is 250 Hz, thus the experimental error in their allocation is around $1/f_{exp} = 4$ ms.

This, if we take as an example the RR intervals, reflects in the calculation of δS and δS_{shuf} errors which are drastically smaller than those required to eventually justify a compatibility of the expression $\overline{\delta S} = 0.76(3)\overline{\delta S}_{shuf}$, obtained from Fig. 9.5(a), with a straight line of slope equal to unity, i.e., $\overline{\delta S} = \overline{\delta S}_{shuf}$.

The difference between δS and δS_{shuf} could be understood in the context that the former depends on the *sequential* order (of beats), while the latter does not.

Since short- (and long-) range correlations is a usual feature (see Ref. [16] and references therein) in heartbeat dynamics, which are possibly destroyed (or become weaker) upon randomizing the data, more "disorder" is intuitively expected to appear after randomization, thus reflecting $\delta S_{shuf} > \delta S$. Furthermore, note that in *all* plots of Fig. 9.5 there are some drastic deviations from the straight line $\overline{\delta S} = \overline{\delta S}_{shuf}$. The origin of some of these deviations will be discussed in Section 9.2.

Finally, by means of a precise example related to SD and H, we further clarify below the aforementioned point that the equality $\overline{\delta S} = \overline{\delta S}_{shuf}$ does *not* necessarily reflect Markovianity.

In Fig. 9.6, we plot for the QT intervals $\overline{\delta S}_{shuf}$ versus $\overline{\delta S}$ (for time-window range 3–10 beats) for SD and H. We see that there are several individuals (mainly SD, see also the next Section) whose values lie practically (i.e., within the error margins) on the straight line $\overline{\delta S} = \overline{\delta S}_{shuf}$. If we plot their δS- (or δS_{shuf}-) values versus the time-window (in a similar fashion as in Fig. 9.2), we find that they are distinctly smaller than those of the Markovian case (note that the δS values in Fig. 9.6 are smaller than 10^{-2}, while those of the Markovian case – depicted in the upper curve in Fig. 9.2 – are $\approx 2 \times 10^{-2}$ or larger). This makes clear that these individuals cannot be characterized as exhibiting Markovian behavior. (This non-Markovianity holds for *all* H and *all* SD.)

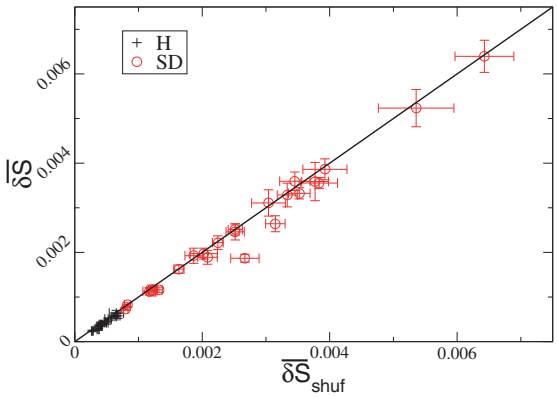

Fig. 9.6 The $\overline{\delta S}$ value, in each of the 10 H (black) and 24 SD (red), for the QT intervals versus $\overline{\delta S}_{shuf}$ (time-window range: 3–10 beats). Note that the values of the ordinates are appreciably smaller than the δS value ($\approx 2 \times 10^{-2}$) of the Markovian time series (10^3 events) depicted in Fig. 9.2. Taken from Ref. [67].

In addition, we note that in Ref. [67] (see § 4.8.3) the difference between δS and δS_{shuf} in the SES activities and "artificial" noises was also studied. It was found (see Table 4.5) that there is a systematic tendency pointing to a value of $\overline{\delta S}_{shuf}/\overline{\delta S}$ larger than unity either for the time-window range 3–5 or for the time-window range 3–10. This is consistent with the non-Markovianity of these signals, thus strengthening the conclusions of § 4.1.2 and § 4.1.3.

9.1.3 Distinction between healthy humans and sudden cardiac death ones by means of either δS(QT) or the ratio $\delta S_{shuf}/\delta S$ of the RR or QRS intervals

We emphasize that, in this subsection, we consider a set consisting *only* of two groups of ECG, namely H and SD. In other words, we are interested here in the distinction of the (otherwise healthy) SD from H, i.e., *if* the population under investigation does *not* include heart disease patients.

First, we point out that in *all* SD, the values of the quantities δS and δS_{shuf} themselves of the QT intervals exceed those of H, see Fig. 9.7. This important distinction between SD and H cannot be attributed (see Sec. VIII of Ref. [63]) to the allocation error of the QT interval.

We now turn to examine whether H and SD can also be distinguished by means of the ratio $\overline{\delta S}_{shuf}/\overline{\delta S}$, which is just the complexity measure ν introduced in § 3.6.1: we calculate this ratio, for each type of interval, at two ranges: (i) a short (s) range 3–4 beats and (ii) a longer (L) range 50–70 beats. By defining $\nu \equiv \overline{\delta S}_{shuf}/\overline{\delta S}$ (see Eq. (3.82)), hereafter the

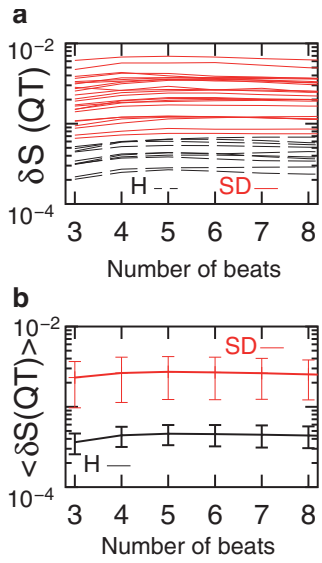

Fig. 9.7 (a) The $\delta S(QT)$ value for each of the 24 SD and 10 H (see Table 9.2) and (b) the average of the δS(QT) values – designated by $\langle \delta S(QT) \rangle$ – along with their standard deviation for each of the two groups SD and H versus the time-window length. Taken from Ref. [68].

following ratios are investigated: $\nu_s(\tau)$ and $\nu_L(\tau)$, where τ denotes the type of interval (i.e., $\tau =$ RR, QRS or QT) and s, L refer to the range studied (i.e., $s =$ 3–4 beats and $L =$ 50–70 beats).

The calculated values for $\nu_s(\tau)$ and $\nu_L(\tau)$ for the three types of intervals are given, for all H and SD, in Table 9.1. The minima $\min_H[\nu_\kappa(\tau)]$ and maxima $\max_H[\nu_\kappa(\tau)]$ (where κ denotes either the short, $\kappa = s$, or the longer, $\kappa = L$, range) among the healthy subjects are also inserted in two separate rows, for each type of interval and each range studied. These minima and maxima are labeled H_{min} and H_{max}, respectively. The cases of SD which have smaller and larger values than H_{min} and H_{max} (reported in each column) are marked with superscripts "*)" and "**)", respectively.

A careful inspection of Table 9.1 leads to the following main conclusion: *all* SD violate one or more *H-limits* (i.e., they have values that are smaller than H_{min} or larger than H_{max}). We intentionally emphasize that this conclusion is also drawn *even* when disregarding the results for the QT intervals. Concerning the latter intervals: Only 5 SD out of 24 violate the *H-limits*; however, in *all* SD, their δS values themselves, as mentioned, are larger than those in H, see also Figs. 9.6 and 9.7. The usefulness of this difference will be discussed later in Section 9.2.

In other words, when focusing our investigation *solely* on the RR and QRS intervals, *all* SD violate one or more of the four *H-limits* related to $\nu_s(RR)$, $\nu_L(RR)$, $\nu_s(QRS)$ and $\nu_L(QRS)$.

This is of profound importance from practical point of view, because the RR and QRS intervals can be detected more easily (and accurately) than the QT by means of an automatic threshold based detector (e.g., see Ref. [22] that evaluated the results of a detector that has been forwarded in Refs. [32] and [30] to determine automatically the waveform limits in Holter ECG).

A further inspection of Table 9.1 leads to the following additional comment:

When investigating the RR intervals *alone* (which can be detected automatically more easily and precisely than the other intervals), i.e., studying $\nu_s(RR)$ and $\nu_L(RR)$, the vast majority of SD (22 out of 24 cases) can be distinguished from H. Only two SD, i.e., sel30 and sel47, obey the corresponding *H-limits*.

Specifically, concerning $\nu_s(RR)$, fifteen SD have values smaller than $H_{min} = 1.18$, while only one SD (i.e., sel43) has a value exceeding $H_{max} = 2.25$. As for $\nu_L(RR)$, eighteen SD exceed $H_{max} = 0.77$, while only 2 SD (i.e., sel34 and sel42) have values smaller than $H_{min} = 0.44$.

9.1.3.1 Tentative physical interpretation of the above results

The main feature of the aforementioned results focuses on the fact that most SD *simultaneously* have $\nu_s(RR)$ values smaller than $H_{min}(= 1.18)$ *and* $\nu_L(RR)$ values exceeding

Table 9.1 The values of the ratios $\overline{\delta S}_{shuf}/\overline{\delta S}$ in the short (s) range 3–4 (ν_s) or in the longer (L) range 50–70 beats (ν_L) in H (sel16265 to sel17453) and SD (sel30 to sel17152) for the RR, QRS and QT intervals. Taken from Ref. [67].

	ν_s, 3–4 beats			ν_L, 50–70 beats		
Individual	RR	QRS	QT	RR	QRS	QT
sel16265	1.82	1.00	1.24	0.48	1.02	0.76
sel16272	1.74	0.99	0.98	0.77	1.08	1.11
sel16273	2.21	1.00	1.48	0.50	0.88	0.71
sel16420	1.55	0.98	1.08	0.53	1.09	0.90
sel16483	2.25	1.02	1.14	0.52	1.16	0.92
sel16539	1.42	1.06	1.25	0.50	1.08	0.65
sel16773	1.94	1.00	0.99	0.44	1.05	0.96
sel16786	1.42	1.00	1.19	0.56	1.04	0.77
sel16795	1.18	0.98	1.08	0.73	0.96	0.99
sel17453	1.38	1.01	1.02	0.56	0.98	0.81
H_{min}	1.18	0.98	0.98	0.44	0.88	0.65
H_{max}	2.25	1.06	1.48	0.77	1.16	1.11
sel30	1.29	1.11**)	1.09	0.65	0.72*)	1.09
sel31	0.96*)	1.08**)	1.17	1.23**)	0.94	0.62*)
sel32	1.39	1.14**)	1.12	1.02**)	0.69*)	0.90
sel33	1.05*)	0.99	1.00	0.86**)	0.82*)	0.99
sel34	2.11	1.29**)	1.11	0.42*)	0.78*)	0.67
sel35	1.00*)	1.00	0.96*)	1.01**)	1.05	1.08
sel36	1.02*)	1.02	1.04	0.92**)	1.00	0.88
sel37	1.07*)	1.18**)	1.07	0.55	0.75*)	0.65
sel38	0.99*)	1.09**)	1.13	1.37**)	0.89	1.04
sel39	0.96*)	1.02	1.06	2.93**)	0.92	0.90
sel40	1.01*)	1.00	0.93*)	0.78**)	0.93	1.29**)
sel41	1.07*)	1.04	1.02	1.07**)	0.84*)	0.96
sel42	1.63	1.08**)	1.23	0.42*)	1.06	0.67
sel43	2.71**)	1.11**)	1.05	0.56	0.76*)	0.89
sel44	0.91*)	0.95*)	0.88*)	2.24**)	1.46**)	1.32**)
sel45	0.98*)	1.24**)	1.29	0.98**)	0.86*)	0.79
sel46	1.03*)	1.01	1.03	1.00**)	0.84*)	1.01
sel47	1.56	0.97*)	1.03	0.45	0.97	1.01
sel48	0.82*)	1.18**)	1.44	1.48**)	0.68*)	0.73
sel49	0.93*)	1.11**)	0.96*)	1.22**)	0.70*)	1.14**)
sel50	1.05*)	0.98	0.98	0.93**)	1.23**)	1.50**)
sel51	1.25	1.01	0.97*)	1.05**)	1.24**)	0.91
sel52	1.50	1.16**)	1.22	1.00**)	0.73*)	0.68
sel17152	1.64	1.01	1.04	0.90**)	1.01	0.97

*) These values are smaller than the minimum (H_{min}) value of $\overline{\delta S}_{shuf}/\overline{\delta S}$ in H for each range.

**) These values are larger than the maximum (H_{max}) value of $\overline{\delta S}_{shuf}/\overline{\delta S}$ in H for each range.

$H_{max}(=0.77)$. The RR time series of healthy subjects are characterized by high complexity (e.g., see Refs. [18, 16]); this, if we recall that in a Markovian series we intuitively expect $\delta S_{shuf}/\delta S = 1$ (and hence $\nu_s = 1$ and $\nu_L = 1$), is compatible with the fact that in *all* H *both* $\nu_s(RR)$ and $\nu_L(RR)$ distinctly differ from unity (see Table 9.1).

We now turn to SD by considering that for individuals at high risk of sudden cardiac death the fractal physiological organization (long-range correlations) breaks down and this is often accompanied by emergence of *uncorrelated randomness*, see Ref. [16] and references therein; see also § 9.2.1.

It is therefore naturally expected that in SD the values of $\nu_s(RR)$ and $\nu_L(RR)$ become closer to the Markovian value (i.e., unity) compared to H. Hence, in SD, $\nu_s(RR)$ naturally becomes smaller than the value 1.18 (the corresponding H_{min}-limit) and $\nu_L(RR)$ larger than 0.77 (the corresponding H_{max}-limit).

We now focus on the following important property of H: although *both* $\nu_s(RR)$ and $\nu_L(RR)$ differ from unity, as mentioned, they systematically behave *differently*, i.e., $\nu_s(RR) > 1$ while $\nu_L(RR) < 1$. The exact origin of the latter difference has not yet been identified with certainty, but the following comments might be relevant: First, in the frame of the frequency-domain characteristics of heart rate variability (e.g., Refs. [38, 49]), we may state that $\nu_s(RR)$ and $\nu_L(RR)$ are associated with the *high-frequency* (HF, 0.15–0.4 Hz) and *low-frequency* (VLF: 0.015–0.04 Hz, LF: 0.04–0.15 Hz) *range in the RR* tachogram ("instantaneous" heart rate, i.e., 1/RR, see also § 9.4.3 and § 9.5.1). An important difference on the effect of the sympathetic and parasympathetic modulation of the RR intervals has been noticed (e.g., see Ref. [38] and references therein): Sympathetic tone is believed to influence the VLF-LF component whereas *both* sympathetic and parasympathetic activity have an effect on the HF component (recall that our results show $\nu_s(RR) > \nu_L(RR)$). Second, at short time-scales (high frequencies), it has been suggested [46] that we have relatively *smooth* heartbeat oscillations associated with respiration (e.g., 15 breaths per minute corresponds to a 4 sec oscillation with a peak in the power spectrum at 0.25 Hz, see Ref. [38]); this is lost upon randomizing the consecutive intervals Q_k, thus probably leading to (larger variations – compared to the original experimental data – between the durations of consecutive intervals and hence to) δS_{shuf} values larger than δS, i.e., a $\nu_s(RR)$ value larger than unity. Such an argument, if true, cannot be applied, of course, in the longer range 50–70 beats and hence explain why the opposite behavior, i.e., $\delta S_{shuf} < \delta S$, then holds. The latter finding must be inherently connected to the nature itself of the long-range correlations. The existence of the latter is evident from the fact that (in this range also) the RR-intervals result in δS values ($\approx 10^{-3}$) which significantly differ from the Markovian δS value ($\approx 10^{-2}$), compare Fig. 9.5(a) with the upper curve in Fig. 9.2.

A simplified interpretation of the results of Fig. 9.6, and in particular the reason why for the QT intervals the quantity δS is larger for the SD than for the H, could be attempted if we consider that: (i) S could be thought as a measure of the "disorder" (in the consecutive intervals) (ii) the essence of the natural time analysis is built on the variation of the durations of consecutive pulses, and (iii) it has been clinically observed (e.g., see Ref. [26]) that the QT interval (which corresponds to the time in which the heart in each beat "re-

covers" – electrically speaking – from the previous excitation) exhibits frequent prolonged values before cardiac death. Thus, when a time-window is sliding on an ECG of H, it is intuitively expected to find, more or less, the same S values (when sweeping through various parts of the ECG) and hence a small δS value is envisaged. By the same token, in an ECG of SD, we expect that, in view of the short–long–short sequences of the QT intervals, the corresponding S values will be much different (compared to H), thus leading to a larger δS value (note that in the same frame we may also understand why the σ/μ values – and hence δS_{shuf}, see Eq. (9.1) – are larger in SD than those in H, as shown in Fig. 9.6).

9.2 Complexity measures of the RR, QRS and QT intervals in natural time to classify sudden cardiac death individuals, heart disease patients and truly healthy ones

9.2.1 Introduction

In complex systems operating far from equilibrium like the case of heart dynamics [16], long-range correlations play an important role (such correlations are also of prominent importance in equilibrium systems when approaching a critical point, e.g., the "critical" temperature T_c, i.e., $T \to T_c$; see Section 1.5). Specifically the existence of long-range correlations in the heart rate variability has been independently established by several applications of DFA, e.g., see Refs. [46, 16] and references therein. Additional studies [21, 18] showed that healthy dynamics exhibits even higher complexity characterized by a broad multifractal spectrum (note that both methods for its determination, i.e., MF-DFA and wavelet transform, see Sections 4.5 and 4.6, respectively, have been employed). This high complexity breaks down in illness and is usually associated with increased mortality in cardiac patients (for more details see § 9.5.1). Thus, in ECG it is advisable that *both* correlations (i.e., short- and long-range), in general, be studied carefully and hence appropriate complexity measures should be envisaged. This is, in simple terms, the physics underlying the procedure that is followed in this Section.

In particular, here we employ the complexity measures introduced in § 3.6.1 to quantify the change of the natural entropy fluctuations at different length scales in time series emitted from systems operating far from equilibrium. Along these lines, we use in ECG the ratios $\delta S_i(RR)/\delta S_j(RR)$, $\delta S_i(QRS)/\delta S_j(QRS)$ and $\delta S_i(QT)/\delta S_j(QT)$ for the RR, QRS and QT intervals, respectively, where i, j denote the time-window length used in the calculation of δS. Assuming that $j < i$, these three ratios provide measures of the δS-*variability* when a scale i changes to a scale j. We select as a common scale (for all RR, QRS and QT) the *smallest* j value reasonable for natural time analysis, i.e., $j = 3$ beats, and for the short-range (s) $i = 5$, while for the longer (L) $i = 60$ beats.

Thus, in accordance to § 3.6.1, the following ratios are studied: $\lambda_s(\tau) \equiv \delta S_5(\tau)/\delta S_3(\tau)$ and $\lambda_L(\tau) \equiv \delta S_{60}(\tau)/\delta S_3(\tau)$, where τ denotes the type of interval, i.e., $\tau =$ RR, QRS or QT.

We also define [68] the ratios

$$\rho_i(\tau) = \delta S_i(RR)/\delta S_i(\tau), \tag{9.3}$$

which provide a *relative* measure of the δS values of the RR intervals compared to either QRS or QT (for the *same* number of beats i). Here, we will use for the short-range $\rho_s(\tau) \equiv \rho_3(\tau)$ and for the long-range $\rho_L(\tau) \equiv \rho_{60}(\tau)$.

Thus, we have 10 complexity measures related to λ and ρ in total: six variability measures, i.e., $\lambda_s(RR)$, $\lambda_L(RR)$, $\lambda_s(QRS)$, $\lambda_L(QRS)$, $\lambda_s(QT)$, $\lambda_L(QT)$, and four relative ones, i.e., $\rho_s(QRS)$, $\rho_L(QRS)$, $\rho_s(QT)$, $\rho_L(QT)$.

We shall show below that these complexity measures identify SD by analyzing fifteen-minute electrocardiograms and comparing them to those of truly healthy humans. In addition, these measures seem to be *complementary* to the ones employed in § 9.1.3, and

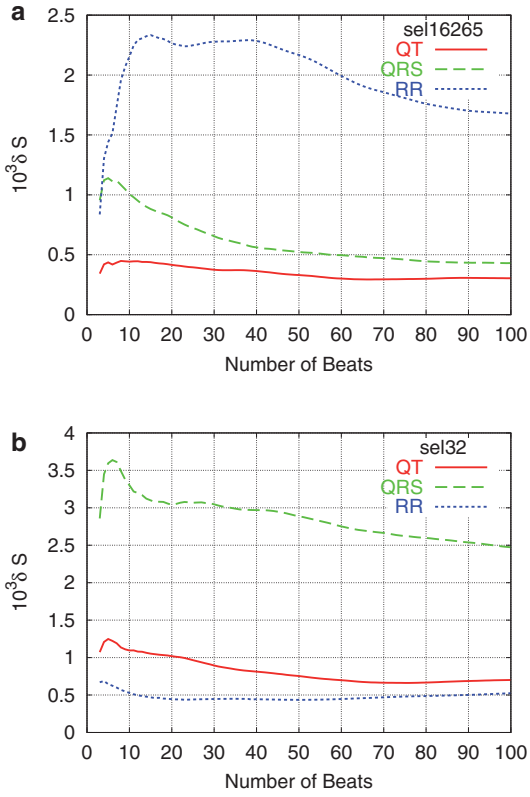

Fig. 9.8 The δS value versus the time-window length for one H (a) and one SD (b). Intervals: QT (solid red), QRS (broken green), and RR (dotted blue). Taken from Ref. [68].

altogether enable the classification of individuals into three categories: H, heart disease patients and SD. We use here the QT-Database of physiobank mentioned in Section 9.1 by considering, beyond the 10H and 24 SD, four groups of heart disease patients, i.e., 15 MIT, 13 MSV, 33 EST and 6 MST. Thus, 101 individuals out of 105 have been investigated (note that the group LT consisting of 4 individuals was discarded in view of its small population). Examples of the δS values, calculated for the RR, QRS and QT intervals in the range 3 to 100 beats are plotted in Figs. 9.8(a) and (b) for one H and one SD, respectively. As for the symbols, we use the same as those mentioned in § 9.1.1.

9.2.2 Distinction of sudden cardiac death individuals (SD) from truly healthy ones (H)

Here, as in § 9.1.3, we consider a set consisting *only* of two groups of ECG, namely H and SD. Thus, we focus here on the distinction of the (otherwise healthy) SD from H, i.e., *if* the population under investigation does *not* include heart disease patients.

The calculated values for the complexity measures $\lambda_\kappa, \rho_\kappa$ (where κ denotes either the short, $\kappa = s$, or the longer, $\kappa = L$, range) are given, for all H and SD, in Table 9.2. The minima $\min_H[\lambda_\kappa(\tau)]$ and maxima $\max_H[\lambda_\kappa(\tau)]$ among the healthy individuals for the RR ($\tau = \text{RR}$) and QRS ($\tau = \text{QRS}$) intervals are also inserted in this Table. We also include the corresponding minima $\min_H[\rho_\kappa(\tau)]$ and maxima $\max_H[\rho_\kappa(\tau)]$ for (the relative δS-variability measure) ρ. For the sake of simplicity, they are labeled H_{min} and H_{max}, respectively, and jointly named *H-limits*. The superscripts 'a' and 'b' show the cases of SD which have smaller and larger values than H_{min} and H_{max}, respectively. In two individuals, i.e., sel41 and sel51, it is uncertain whether their measure $\lambda_s(QRS)$ violates the value $H_{min} = 1.15$.

Table 9.2 reveals that *all* SD violate one or more *H-limits* of the four complexity measures $\lambda_s(RR)$, $\lambda_L(RR)$, $\rho_s(QRS)$ and $\rho_L(QRS)$, and hence can be distinguished from H.

In other words, the δS-variability measures of the RR-intervals, together with their relative ones with respect to the QRS (i.e., four parameters in total), seem to achieve a distinction between SD and H.

Note that $\lambda_\kappa(RR)$ *alone* can classify the vast majority of SD, i.e, all SD except sel47. Furthermore, attention is drawn to the point that if we also consider the $\lambda_\kappa(\tau)$ values calculated (*not* in the original, but) in the randomized ("shuffled") sequence of Q_m, we find that *all* SD violate one or more *H-limits* of $\lambda_\kappa(RR)$ and $\lambda_{\kappa,shuf}(RR)$ (see Table 9.2 and table VII of Ref. [63], respectively). This allows using again four parameters in total the distinction of *all* SD from H by using the RR intervals *only*.

Thus, we found that among the 10 parameters defined in the original time series extracted from each ECG (or 20 parameters, in total, if we also account for the correspond-

Table 9.2 The variability measures (λ), the relative ones (ρ), and the ratios $\nu \equiv \overline{\delta S}_{shuf}/\overline{\delta S}$ in the short (s) range and in the longer (L) range in H (sel16265 to sel17453) and SD (sel30 to sel17152) along with their $\overline{\delta S}_{3-4}(QT)$ values. Taken from Ref. [68].

Individual	RR		QRS		QT		RR over QRS	
	$\lambda_s(RR)$	$\lambda_L(RR)$	$\lambda_s(QRS)$	$\lambda_L(QRS)$	$\lambda_s(QT)$	$\lambda_L(QT)$	$\rho_s(QRS)$	$\rho_L(QRS)$
sel16265	1.72	2.38	1.19	0.52	1.27	0.88	0.88	4.01
sel16272	1.69	1.35	1.29	0.61	1.21	0.50	0.18	0.40
sel16273	1.61	2.69	1.16	0.59	1.30	1.11	1.11	5.05
sel16420	1.51	1.74	1.22	0.48	1.37	0.66	0.96	3.46
sel16483	1.43	2.37	1.23	0.49	1.31	0.68	0.25	1.22
sel16539	2.00	1.94	1.26	0.50	1.41	1.08	1.85	7.10
sel16773	1.92	2.61	1.21	0.49	1.31	0.70	0.90	4.84
sel16786	1.71	1.57	1.19	0.51	1.31	0.84	1.16	3.56
sel16795	1.77	0.99	1.24	0.55	1.16	0.56	0.77	1.37
sel17453	1.87	1.67	1.26	0.54	1.22	0.68	1.49	4.59
H_{min}	1.43	0.99	1.16	0.48	1.16	0.50	0.18	0.40
H_{max}	2.00	2.69	1.29	0.61	1.41	1.11	1.85	7.10
sel30	1.11[a]	0.89[a]	1.20	1.05[b]	1.28	0.56	0.51	0.43
sel31	0.96[a]	0.34[a]	1.39[b]	0.89[b]	1.30	0.84	1.10	0.42
sel32	0.96[a]	0.67[a]	1.26	0.96[b]	1.16	0.65	0.23	0.16[a]
sel33	1.14[a]	0.77[a]	0.96[a]	0.52	1.21	0.53	0.79	1.17
sel34	1.87	3.04[b]	1.33[b]	1.22[b]	1.15[a]	0.85	0.40	1.00
sel35	1.12[a]	0.52[a]	1.24	0.66[b]	1.12[a]	0.44[a]	1.72	
sel36	1.31[a]	0.62[a]	1.12[a]	0.51	1.26	0.60	2.35[b]	2.88
sel37	0.92[a]	0.71[a]	1.26	0.87[b]	1.11[a]	0.78	0.71	0.58
sel38	0.91[a]	0.34[a]	1.27	0.65[b]	1.03[a]	0.50	0.65	0.34[a]
sel39	0.81[a]	0.11[a]	1.23	0.72[b]	1.17	0.58	0.80	0.12[a]
sel40	1.66	0.81[a]	1.14[a]	0.55	1.19	0.43[a]	0.12[a]	0.18[a]
sel41	1.14[a]	0.48[a]	1.18	0.70[b]	1.22	0.56	0.21	0.15[a]
sel42	1.10[a]	1.81	1.16	0.51	1.31	1.01	0.95	3.40
sel43	1.69	3.04[b]	1.24	0.77[b]	1.26	0.68	0.06[a]	0.23[a]
sel44	1.18[a]	0.18[a]	1.52[b]	0.43[a]	1.02[a]	0.34[a]	0.59	0.25[a]
sel45	0.92[a]	0.42[a]	1.16	0.73[b]	1.37	0.68	1.46	0.85
sel46	0.94[a]	0.43[a]	1.05[a]	0.71[b]	1.12[a]	0.55	1.35	0.82
sel47	1.54	2.07	1.19	0.54	1.36	0.57	0.16[a]	0.63
sel48	0.84[a]	0.30[a]	1.23	1.08[b]	1.14[a]	1.00	0.91	0.26[a]
sel49	0.93[a]	0.33[a]	1.17	0.83[b]	1.16	0.50	1.27	0.50
sel50	1.32[a]	0.59[a]	1.28	0.46[a]	1.21	0.32[a]	1.78	2.31
sel51	1.83	0.72[a]	1.14[a]	0.42[a]	1.24	0.66	0.16[a]	0.27[a]
sel52	1.40[a]	0.73	1.32[b]	1.02[b]	1.29	1.01	0.14[a]	0.10[a]
sel17152	1.06[a]	0.93[a]	1.31[b]	0.58	1.13[a]	0.54	0.06[a]	0.10[a]
min	0.81	0.11	0.96	0.42	1.02	0.32	0.06	0.10
max	1.87	3.04	1.52	1.22	1.37	1.01	2.35	3.40

Table 9.2 Continued

RR over QT		3–4 beats (ν_s)[c]			50–70 beats (ν_L)[c]			
$\rho_s(QT)$	$\rho_L(QT)$	RR	QRS	QT	RR	QRS	QT	$\overline{\delta S}_{3-4}(QT) \times 10^3$
2.44	6.62	1.87	0.98	1.29	0.48	1.02	0.75	0.38
0.67	1.79	1.65	0.88	0.94	0.77	1.10	1.07	0.48
3.17	7.65	2.18	0.99	1.46	0.50	0.88	0.71	0.24
1.97	5.21	1.60	0.99	1.07	0.53	1.09	0.90	0.36
0.96	3.37	2.27	0.99	1.17	0.52	1.15	0.92	0.35
5.57	10.04	1.43	1.07	1.27	0.50	1.08	0.65	0.52
1.49	5.54	1.85	1.01	0.91	0.44	1.05	0.97	0.55
3.97	7.43	1.39	1.01	1.19	0.55	1.04	0.77	0.23
2.87	5.08	1.10	0.98	1.05	0.74	0.95	1.00	0.56
2.91	7.12	1.46	1.01	1.02	0.57	0.98	0.81	0.34
0.67	1.79	1.10	0.88	0.91	0.44	0.88	0.65	0.23
5.57	10.04	2.27	1.07	1.46	0.77	1.15	1.07	0.56
1.73	2.73	1.15	1.08[b]	1.13	0.66	0.71[a]	1.10[b]	1.04[b]
0.80	0.32[a]	0.90[a]	1.06	1.15	1.23[b]	0.97	0.63[a]	3.01[b]
0.63[a]	0.64[a]	1.31	1.11[b]	1.13	1.02[b]	0.69[a]	0.90	1.14[b]
2.41	3.50	1.07[a]	1.00	1.08	0.85[b]	0.83[a]	1.00	0.76[b]
1.16	4.12	2.13	1.11[b]	1.12	0.41[a]	0.77[a]	0.67	0.69[b]
0.83	0.99[a]	1.02[a]	0.97	0.97	1.02[b]	1.05	1.07	6.45[b]
1.45	1.52[a]	1.03[a]	1.01	1.08	0.93[b]	0.99	0.89	2.08[b]
1.19	1.07[a]	1.11	1.17[b]	1.07	0.56	0.75[a]	0.64[a]	3.30[b]
0.37[a]	0.25[a]	1.15	1.08	1.12	1.33[b]	0.89	1.03	2.71[b]
1.53	0.28[a]	0.97[a]	0.97	0.99	2.93[b]	0.93	0.89	2.44[b]
0.20[a]	0.38[a]	1.03[a]	1.01	0.93	0.79[b]	0.94	1.30[b]	3.43[b]
0.80	0.68[a]	0.91[a]	1.04	1.06	1.05[b]	0.84[a]	0.96	1.53[b]
1.62	2.89	1.63	1.09[b]	1.26	0.43[a]	1.06	0.66	0.95[b]
0.11	0.48[a]	2.79[b]	1.12[b]	1.08	0.56	0.77[a]	0.89	2.23[b]
1.08	0.58[a]	0.91[a]	0.92	0.90[a]	2.25[b]	1.46[b]	1.33[b]	4.12[b]
1.14	0.71[a]	0.97[a]	1.05	1.11	0.98[b]	0.88	0.79	1.71[b]
1.59	1.26[a]	1.01[a]	0.99	1.01	0.99[b]	0.85[a]	1.01	3.44[b]
0.14[a]	0.49[a]	1.60	0.97	0.97	0.45	0.96	1.02	2.85[b]
1.36	0.41[a]	0.84[a]	1.24[b]	1.42	1.49[b]	0.68[a]	0.74	1.75[b]
1.08	0.71[a]	0.86[a]	1.15[b]	0.96	1.21[b]	0.71[a]	1.11[b]	3.96[b]
1.21	2.26	1.07[a]	1.00	0.91	0.93[b]	1.20[b]	1.62[b]	5.21[b]
0.30[a]	0.33[a]	1.30	1.04	1.00	1.05[b]	1.24[b]	0.90	1.83[b]
0.42[a]	0.31[a]	1.51	1.13[b]	1.17	1.02[b]	0.73[a]	0.67	1.66[b]
0.23[a]	0.40[a]	1.68	1.01	1.03	0.91[b]	1.01	0.97	1.15[b]
0.11	0.25	0.84	0.92	0.90	0.41	0.68	0.63	0.69
2.41	4.12	2.79	1.24	1.42	2.93	1.46	1.62	6.45

a) These values are smaller than the H_{min} given in each column.
b) These values are larger than the H_{max} given in each column.
c) These values do not fully coincide with those given in Ref. [67] for the reasons discussed in § 9.2.7.

ing parameters defined in the time series obtained after shuffling the Q_m randomly), *only* four are required for the distinction between SD and H. We clarify that this seems to be extremely difficult to be achieved by chance. In order to visualize it, if we assume (for the sake of convenience only) independent and identically distributed (i.i.d.) values of the parameters for one subject, we find that the probability that *all* 4 parameters are within the bounds (minima and maxima) set by 10 other subjects (i.e., the healthy ones) is $(1-2/11)^4 \approx 0.448$. Thus, the probability that all 24 additional subjects are classified as SD by pure chance is $(1-0.448)^{24} \approx 6.4 \times 10^{-7}$, i.e., extremely small (note that only if one decides which parameters one wants to use *before* the calculation of the values is this probability valid; this is the reason why blind evaluation – defining all methods, parameters and criteria studying one set of data, and *then* testing the significance using an additional set of independent data – is considered very important in medical applications and/or publications). If one just picks 4 parameters out of the original 20 as in our case, the above probability should be multiplied by the possible combinations of selecting 4 objects among 20, i.e., $20!/(4!16!) = 4{,}845$, leading to a value 0.31% of achieving our result by chance.

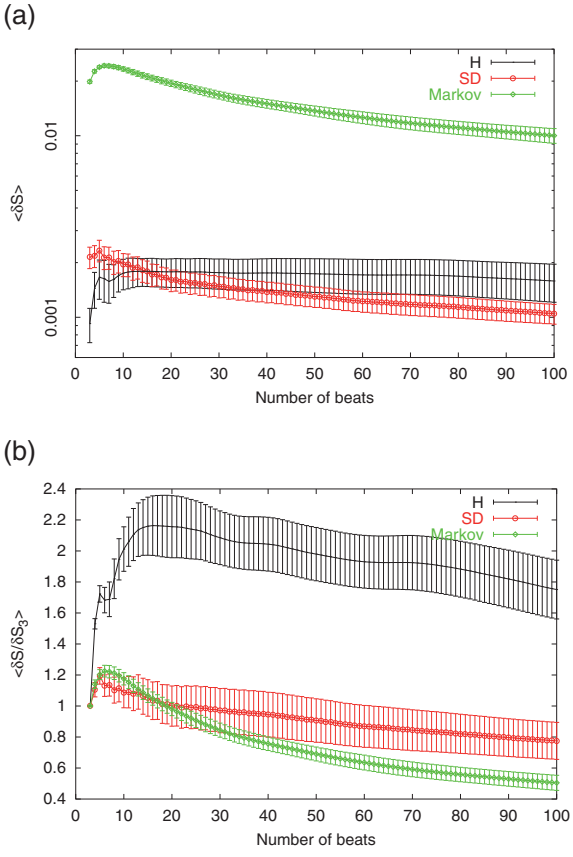

Fig. 9.9 The average (denoted by the brackets) values of (a): the $\delta S_i(RR)$ and (b): $\delta S_i(RR)/\delta S_3(RR)$ for the SD (solid black) and H (red circles) versus the time-window length; the bars correspond to the standard error of the mean. The results for a Markovian time series are also plotted (green squares), but the bars here denote the standard deviation. Taken from Ref. [68].

9.2.2.1 Physical interpretation of the aforementioned results in § 9.2.2

The main feature of these results focuses on the fact that both ratios $\lambda_s(RR)$ and $\lambda_L(RR)$ become smaller in the vast majority of SD, compared to H.

Recall that the $\delta S_i(RR)$ values themselves cannot distinguish SD from H, see Fig. 9.9(a), in contrast to the ratios $\delta S_i(RR)/\delta S_3(RR)$, see Fig. 9.9(b).

We now consider that for individuals at high risk of sudden cardiac death, the fractal organization (long-range correlations) that characterizes the healthy subjects breaks down (see Refs. [18, 15] and references therein; see also § 9.2.1 and § 9.5.1). This breakdown is often accompanied by emergence of *uncorrelated randomness* (as already mentioned in § 9.1.3.1) or *excessive* order (e.g., periodic oscillations appear in the heart rate recordings of "frequency" $\approx$ 1/min, which are associated with Cheyne–Stokes breathing) [15].

Let us now calculate [67] the δS values in a (dichotomous) Markovian (hereafter labeled $\mathscr{M}$) time series (exponentially distributed durations), see § 9.1.2, hereafter labeled $\delta S_i(\mathscr{M})$, for a total number of $N = 10^3$ pulses (i.e., length comparable to that of the ECG analyzed here). These values are plotted – along with those for SD and H – in green in Fig. 9.9(a) and show that the corresponding λ_s and λ_L variability measures are

$$\lambda_s(\mathscr{M}) = 1.20 \pm 0.03 \ \text{ and } \ \lambda_L(\mathscr{M}) = 0.64 \pm 0.05; \tag{9.4}$$

see Fig. 9.9(b). Three comments are now in order:

First, the $\delta S_i(\mathscr{M})$ values differ drastically, see Fig. 9.9(a), from the $\delta S_i(RR)$ values themselves of *both* SD and H, which indicates that the RR intervals (both in SD and H) exhibit non-Markovian behavior, as mentioned in § 9.1.2.

This is consistent with the aspects that bodily rhythms, such as the heartbeat, show complex dynamics, e.g., Refs. [18, 15].

Second, the fact that $\lambda_s(RR)$ in SD becomes smaller than in H can now be understood as follows: Since H exhibit a high degree of complexity, it is expected that (even) their H_{min} value (= 1.43) should markedly exceed $\lambda_s(\mathscr{M})$. On the other hand, in SD this high complexity breaks down and hence their $\lambda_s(RR)$ values naturally approach $\lambda_s(\mathscr{M})$, thus becoming smaller.

This is strengthened by the fact that the SD average value of $\lambda_s(RR)$ in Table 9.2 is 1.19, which almost coincides with $\lambda_s(\mathscr{M})(= 1.20)$.

The latter coincidence also occurs for the QRS intervals in *both* H and SD, which agrees with the observations [26] mentioned above (§ 9.1.3.1) that the prolonged QT intervals in SD mainly originate from enlarged ST values, while their QRS intervals may remain the *same*.

Third, we now turn to the interpretation of the results related to $\lambda_L(RR)$. In H, it is expected that (in view of the RR long-range correlations [15]) the corresponding values must be appreciably larger than $\lambda_L(\mathscr{M}) = 0.64 \pm 0.05$. We now examine the SD: If, in SD "*uncorrelated randomness*" appears, this reflects that their $\lambda_L(RR)$ values naturally approach $\lambda_L(\mathscr{M})$, thus becoming smaller (compared to H); this actually occurs in the vast majority of SD in Table 9.2.

If in SD the aforementioned periodicities (associated with Cheyne–Stokes breathing) appear, it is naturally expected (as shown below in § 9.2.2.2) to find *large* δS values when a time-window of length around 60 beats, or so (i.e., related to the aforementioned "frequency" $\approx$ 1/min) sweeps through the RR time series. This for SD, results in δS values even larger than those in H, since in H no such periodicities appear, as actually observed in the *two* cases marked with superscript 'b' (i.e., those exceeding H_{max}) in Table 9.2.

The plausibility of the above interpretation is considerably strengthened by the following remarks. Recall that the H_{min} values for $\lambda_s(RR)$ and $\lambda_L(RR)$ have been determined *empirically* by selecting the smallest values among the 10 H. We may overcome this empirical selection, however, as follows. We divide each ECG in equal and non-overlapping segments of length (l) significantly larger than the time-window of 60 beats (e.g., $l = 180$ or 120 beats; see Tables 9.3 and 9.4, respectively) and calculate the corresponding measures $[\lambda_s(RR)]_l$ and $[\lambda_L(RR)]_l$ for the various segments labeled by l. The mean values $\langle \lambda_\kappa(RR) \rangle_l$ for each individual, agree more or less with the values that have been obtained above, when the time-window swept through the whole record and their standard deviations provide a measure of the variability of each of these two complexity measures among the various segments studied in each record. Comparing the values of $\min\{[\lambda_s(RR)]_l\}$ and $\min\{[\lambda_L(RR)]_l\}$ (see the Tables 9.3 and 9.4) to $\lambda_s(\mathscr{M})$ and $\lambda_L(\mathscr{M})$, respectively, we find the following. In H , the values of $\min\{[\lambda_\kappa(RR)]_l\}$ significantly exceed $\lambda_\kappa(\mathscr{M})$ for $\kappa = s$ or L, as they should (with a possible exception of $\min\{[\lambda_L(RR)]_l\}$ for sel16795, which might be due to the fact that the ECG of this individual has the smallest length, i.e., 760 beats, among the H). On the other hand, most SD (e.g., in Table 9.3 those marked with 'c' and 'd') exhibit $\min\{[\lambda_\kappa(RR)]_l\}$ values which are smaller than (or equal to) $\lambda_\kappa(\mathscr{M})$ for $\kappa = s$ or L (the values in bold, in both Tables 9.3 and 9.4, indicate the minority of cases of SD in which the resulting $\min\{[\lambda_\kappa(RR)]_l\}$ values exceed $\lambda_\kappa(\mathscr{M})$). Interestingly, all these (21 or 22 out of 24) SD cases coincide with those already marked with 'a' in Table 9.2 on the basis of the empirically determined *H-limits* of $\lambda_s(RR)$ and $\lambda_L(RR)$. Thus, the essence of our findings could be summarized as follows:

When a time-window sweeps through the *whole* record available, the vast majority of SD exhibits $\lambda_s(RR)$ and $\lambda_L(RR)$ values which are significantly smaller than those in H and hence SD are distinguished from H. This finding stems from the fact that some segments of the SD records exhibit values of these measures that are comparable with those of a Markovian behavior (see Fig. 9.9(b)).

Table 9.3 The resulting values of the *variability* measures $\lambda_s(RR)$ and $\lambda_L(RR)$ when using segments of length $l = 180$ beats and then calculating their mean and minimum values. Taken from Ref. [63].

Signal	$\lambda_s(RR)$				$\lambda_L(RR)$			
	$\lambda_s(RR)^{a)}$	$\lambda_s(RR)^{b)}$	$\langle\lambda_s(RR)\rangle_l$	$\min\{[\lambda_s(RR)]_l\}$	$\lambda_L(RR)^{a)}$	$\lambda_L(RR)^{b)}$	$\langle\lambda_L(RR)\rangle_l$	$\min\{[\lambda_L(RR)]_l\}$
sel16265	1.72	1.73	1.69	1.52	2.38	2.40	1.78	0.92
sel16272	1.69	1.66	1.67	1.56	1.35	1.44	1.31	1.12
sel16273	1.61	1.60	1.60	1.52	2.69	2.67	2.50	1.11
sel16420	1.51	1.54	1.50	1.43	1.74	1.80	1.80	1.37
sel16483	1.43	1.38	1.40	1.30	2.37	2.51	2.19	1.44
sel16539	2.00	2.10	2.02	1.73	1.94	2.08	1.92	1.03
sel16773	1.92	1.93	1.90	1.66	2.61	2.64	2.26	1.52
sel16786	1.71	1.78	1.76	1.54	1.57	1.70	1.51	0.95
sel16795	1.77	1.81	1.77	1.67	0.99	1.10	0.82	0.41[e)]
sel17453	1.87	1.91	1.90	1.85	1.67	1.73	1.68	0.93
sel30	1.11[c)]	1.12	1.17	1.03	0.89	1.06	1.38	**1.21**
sel31	0.96[c)]	0.96	0.97	0.88	0.34[d)]	0.34	0.35	0.28
sel32	0.96[c)]	1.12	1.28	0.93	0.67[d)]	0.95	1.32	0.39
sel33	1.14[c)]	0.90	1.07	0.92	0.77	0.74	0.87	**0.77**
sel34	1.87	2.07	1.99	**1.50**	3.04	3.48	2.82	**1.32**
sel35	1.12[c)]	1.13	1.14	1.07	0.52[d)]	0.58	0.56	0.44
sel36	1.31[c)]	1.30	1.33	1.16	0.62[d)]	0.63	0.64	0.48
sel37	0.92[c)]	0.91	0.94	0.75	0.71[d)]	0.78	0.69	0.51
sel38	0.91[c)]	0.81	1.09	0.79	0.34[d)]	0.12	0.36	0.08
sel39	0.81[c)]	0.81	0.81	0.79	0.11[d)]	0.11	0.10	0.07
sel40	1.66	1.16	1.65	**1.60**	0.81[d)]	0.82	0.67	0.35
sel41	1.14[c)]	1.13	1.31	0.91	0.48[d)]	0.44	0.63	0.10
sel42	1.10[c)]	1.22	1.31	0.87	1.81[d)]	2.13	2.59	0.69
sel43	1.69	1.55	1.63	**1.52**	3.04	3.85	3.24	**1.65**
sel44	1.18[c)]	1.17	1.19	1.17	0.18[d)]	0.18	0.17	0.13
sel45	0.92[c)]	0.92	1.12	0.82	0.42[d)]	0.42	0.65	0.11
sel46	0.94[c)]	0.96	0.94	0.88	0.43[d)]	0.46	0.41	0.30
sel47	1.54	1.54	1.54	**1.37**	2.07	2.16	2.32	**1.81**
sel48	0.84[c)]	0.84	0.93	0.84	0.30[d)]	0.30	0.79	0.14
sel49	0.93[c)]	0.89	0.93	0.87	0.33[d)]	0.37	0.32	0.20
sel50	1.32[c)]	1.33	1.33	1.16	0.59[d)]	0.73	0.61	0.49
sel51	1.83	1.87	1.79	**1.63**	0.72[d)]	0.75	0.77	0.66
sel52	1.40[c)]	1.41	1.13	0.99	0.73[d)]	0.74	0.69	0.49
sel17152	1.06[c)]	0.94	1.00	0.87	0.93[d)]	0.98	1.12	0.51

a) They come from Table 9.2.

b) These values, for the sake of comparison, are obtained after applying a detection algorithm which excludes the "outliers"; this algorithm is analogous to the one used by Ivanov et al. [21].

c) These individuals have $\min\{[\lambda_s(RR)]_l\}$ values which are equal to or smaller than the value $\lambda_s(\mathscr{M}) = 1.20 \pm 0.03$ discussed in the text.

d) These individuals have $\min\{[\lambda_L(RR)]_l\}$ values which are equal to or smaller than the value $\lambda_L(\mathscr{M}) = 0.64 \pm 0.05$ discussed in the text.

e) The ECG of this individual has the smallest length (760 beats) among the H, which might be one of the reasons why this case only deviates from the other H.

Table 9.4 The resulting values of the *variability* measures $\lambda_s(RR)$ and $\lambda_L(RR)$ when using segments of length $l = 120$ beats and then calculating their mean and minimum values. Taken from Ref. [63].

Signal	$\lambda_s(RR)$		$\lambda_L(RR)$	
	$\langle\lambda_s(RR)\rangle_l$	$\min\{[\lambda_s(RR)]_l\}$	$\langle\lambda_L(RR)\rangle_l$	$\min\{[\lambda_L(RR)]_l\}$
sel16265	1.70	1.46	1.87	0.98
sel16272	1.66	1.46	1.20	0.82
sel16273	1.59	1.47	1.95	0.79
sel16420	1.51	1.39	1.57	0.86
sel16483	1.42	1.23	2.45	0.90
sel16539	2.04	1.67	1.50	0.90
sel16773	1.91	1.67	2.41	0.77
sel16786	1.78	1.49	1.18	0.69
sel16795	1.77	1.68	0.68	0.44[e)]
sel17453	1.93	1.77	1.33	0.77
sel30	1.09	0.93	1.02	0.68
sel31	0.99	0.87	0.31	0.19
sel32	1.34	0.92	1.82	0.27
sel33	1.13	0.91	0.70	0.46
sel34	2.01	**1.39**	2.92	**1.26**
sel35	1.15	1.03	0.45	0.35
sel36	1.33	1.21	0.64	0.36
sel37	0.96	0.75	0.53	0.33
sel38	1.11	0.78	0.34	0.07
sel39	0.81	0.78	0.10	0.06
sel40	1.66	**1.58**	0.64	0.23
sel41	1.32	0.88	0.58	0.18
sel42	1.43	0.81	2.31	0.48
sel43	1.62	**1.42**	3.39	**1.11**
sel44	1.19	1.13	0.16	0.09
sel45	1.17	0.81	0.69	0.19
sel46	0.94	0.85	0.41	0.29
sel47	1.55	**1.34**	1.83	**1.28**
sel48	0.98	0.77	1.64	0.14
sel49	0.91	0.86	0.25	0.08
sel50	1.32	1.09	0.51	0.34
sel51	1.80	**1.60**	0.63	0.57
sel52	1.11	0.94	0.72	0.29
sel17152	0.99	0.79	1.16	0.40

[e)] The ECG of this individual has the smallest length (760 beats) among the H, which might be one of the reasons why this case only deviates from the other H.

The same conclusions are drawn irrespective of whether we use a detection algorithm to exclude 'outliers' from the records. In the third column (labeled with a superscript 'b') of Table 9.3, we present the values obtained after applying such a detection algorithm. More precisely a moving window average filter was applied. For each set of five contiguous intervals, a local mean was computed, excluding the central interval. If the value of the central interval exceeded the local average by a factor 1.5 or larger, it was considered to

be an outlier and excluded from the interval series. This algorithm is analogous to the one used by Ivanov et al. [21].

9.2.2.2 Study of the δS values for time series with a "sinusoidal" background

In Fig. 9.10, we show the δS value calculated when a time-window of length 3–100 beats is sliding through the time series given by

$$x_k = a + b\,\sin(2\pi k/T), \tag{9.5}$$

or

$$y_k = \mu + \sigma\,\sin(2\pi k/T)\eta, \tag{9.6}$$

where η is an exponentially distributed random variable of unit mean and standard deviation. The amplitude of the "oscillation" b or σ is comparable to the standard deviation of the RR intervals in ECG and the "period" T is 60 beats, i.e., comparable to that of the periodic oscillations in the heart rate recordings which are associated with Cheyne–Stokes breathing [15] mentioned above in § 9.2.2.1. The main result of Fig. 9.10 could be summarized as follows:

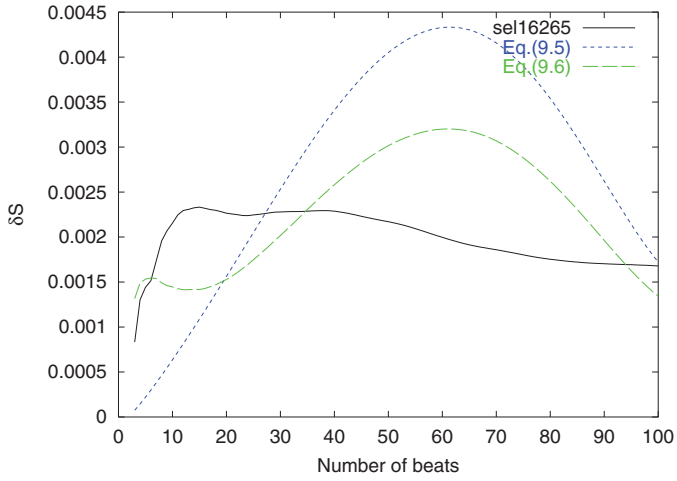

Fig. 9.10 The δS values versus the time-window length for one H (sel16265) together with those obtained using Eq. (9.5) (dotted blue) or Eq. (9.6) (broken green). Note that *no* maximum at around 60 beats appears in the case of H. Taken from Ref. [63].

When the length of the sliding time-window becomes equal to the "period" ($T = 60$ beats) of the "oscillating" background, the δS value becomes maximum.

Note that the window length corresponding to the maximum amplitude is practically equal to that observed *if* the "oscillating" background were *solely* present; the latter case for the sake of comparison is also plotted in dotted blue in Fig. 9.10.

9.2.3 Comparison of the present results in natural time with those deduced from the Approximate Entropy (AE) or the Sample Entropy (SE) to distinguish SD from H

In § 9.1.1, it was mentioned that two other dynamic entropies, i.e., AE or SE, have been applied to ECG analysis. Here, we compare [63] the results of these two entropies to distinguish SD from H with those achieved above in § 9.2.2 by means of the complexity measures in natural time.

AE and SE are based on two input parameters: the sequence length m and the tolerance level r. The smallest values of entropy correspond to perfectly regular sequences, since the output of these algorithms provides a likelihood measure that two sequences (within tolerance level r) remain close at the next point. Note that as r decreases both AE and SE increase, because the criterion for sequence matching becomes more stringent [51].

In Fig. 9.11, we plot the values of AE calculated for $r = 0.2$STD and $m = 2$ (as recommended in the program `apen` [25]) and SE, again for $m = 2$, and $r = 0.2$STD (by means of the program `sampen` [33]) along with the values of the entropy S in natural time for SD and H.

Note that no distinction of *all* individuals can be achieved by means of either AE or SE (note that this still holds if we calculate AE for $r = 0.65$STD as recommended in Ref. [44]), although the average values of the two groups actually turn out to be different. This shows the necessity of using the complexity measures based on the fluctuations δS of the entropy S in natural time in order to obtain the distinction of *all* SD from H as in § 9.1.3 and § 9.2.2. Such a distinction cannot be achieved by means of the S values themselves (which are close to S_u, see Fig. 9.11) as already emphasized in § 9.1.1.

9.2.4 The procedure for identifying SD among other individuals that include healthy ones and heart disease patients

We first address the question of distinguishing all SD from the other individuals (heart disease patients and H).

We use here the 101 individuals mentioned in § 9.2.1.

The values of all the complexity measures in natural time: λ, ρ, ν,$\overline{\delta S}_{3-4}$(QT), λ_{shuf}, ρ_{shuf} and $\overline{\delta S}_{3-4,shuf}$(QT) for each one of the 101 ECG can be found in Table 9.2 and in tables III to VII of Ref. [63] which are freely accessible.

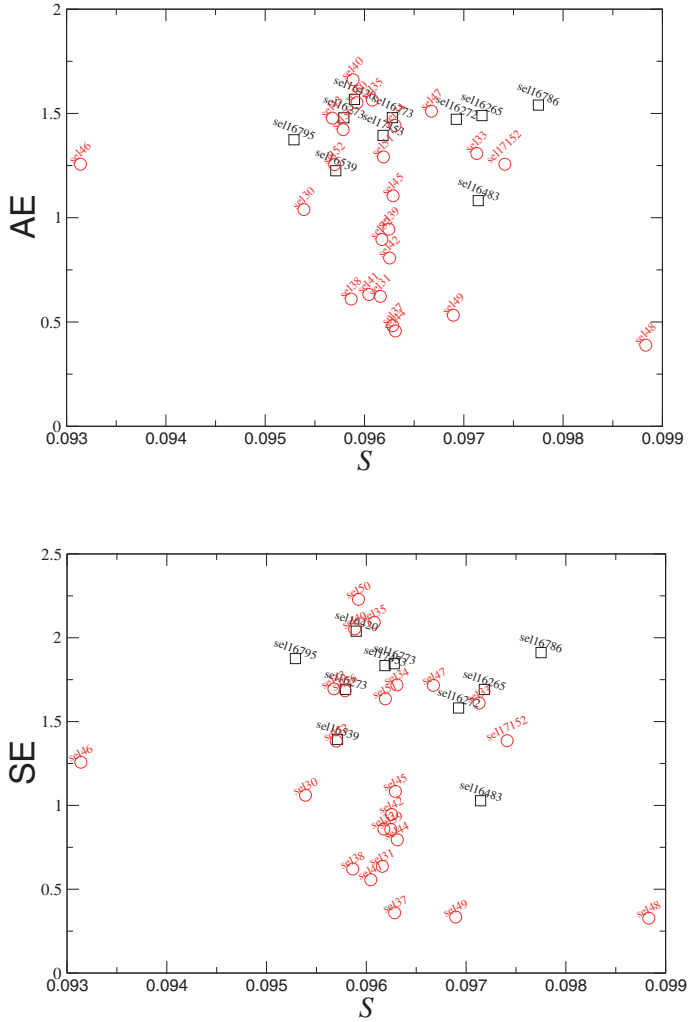

Fig. 9.11 The values (for $m = 2$, $r = 0.2$STD) of AE (upper panel) or SE (lower panel) versus the entropy S in natural time calculated for SD and H. Taken from Ref. [63].

In addition, the quality of ECG data was discussed in Ref. [63] with the following results: Among the 101 individuals investigated, five patients have been identified as "outliers". The appearance of such "outliers" is not surprising (see below) when using (as we did) an automatic threshold detector [31, 22, 32, 30] for the allocation of the intervals. More precisely, their recognition was made as follows: four individuals, i.e., two MIT (sel230 and sel231) and two EST (sele0612 and sele0704), have been identified as "outliers", because they exhibit $\nu_s(QRS)$ values which are *unusually* larger than unity (a simple statistical test – by means of the STATIST [39] – of the 101 $\nu_s(QRS)$ values, immediately shows that these four cases can be considered as "outliers"). The fifth individual identified

as "outlier", i.e., sele0136, has a $\rho_L(QRS)$ value drastically larger than the corresponding values of *all* other patients.

An inspection of the measures λ, ρ, ν shows three facts. First, *all* SD and *all* patients violate one or more *H-limits*. Second, *none* of the measures λ, ρ, ν alone, or a combination of two of them, can effectively differentiate the SD from the patients. Third, if we consider the three measures λ, ρ, ν (i.e., 16 parameters consisting of the 10 parameters explained in § 9.2.1 and the 6 parameters of ν_s and ν_L related to the RR, QRS and QT intervals, e.g., see Table 9.1) altogether, we find that 20 SD out of 24 violate some of the limits of both patients and H, thus allowing in principle a distinction of the *vast* majority of SD from the other individuals.

Thus, in summary, the consideration of the quantities (λ, ρ, ν) *only*, does not lead to a distinction of *all* SD from the patients. The same conclusion is drawn if we alternatively consider the quantities (λ, λ_{shuf},ρ) *only*.

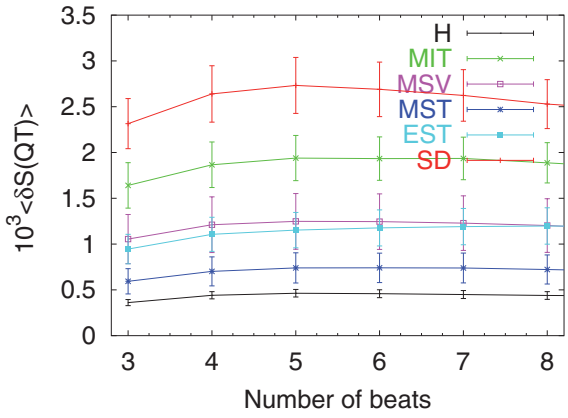

Fig. 9.12 The average of the $\delta S(QT)$ values – labeled $\langle \delta S(QT) \rangle$ – for each of the six groups labeled H, MIT, MSV, MST, EST and SD versus the time-window length. The bars denote the standard error of the mean. (The corresponding standard deviations overlap considerably and hence are not shown for the sake of clarity.) The lowermost curve and the uppermost curve correspond to H and SD, respectively and hence coincide with the two curves depicted in Fig. 9.7(b). Taken from Ref. [68].

We now turn to the investigation of the δS(QT) values, which as shown in Fig 9.7(a) allows the distinction of *all* SD from H. In Fig. 9.12, the average value $\langle \delta S \rangle$(QT) for each group is plotted versus the time-window length. It is intriguing that the results of the four groups (MIT, MSV, MST, EST) of patients are located between H (the lowermost curve) and SD (the uppermost curve). We emphasize, however, that if we plot the curves for each one of the 101 individuals (in a way similar to that of Fig. 9.7(a)), we find that there are some patients whose results overlap with either SD or H. We now restrict ourselves to $\overline{\delta S}_{3-4}$(QT) which for the sake of simplicity will be hereafter simply denoted δS(QT). Let us consider only the limiting cases – i.e., the values corresponding to the lowermost and the uppermost curve, to be called hereafter $\delta S(\mathrm{QT})_{min,\xi}$ and $\delta S(\mathrm{QT})_{max,\xi}$, respectively – obtained in each group ξ of heart disease patients, i.e., ξ = MIT, MSV, EST or MST. In order to distinguish SD from heart disease patients, we must appropriately discriminate the overlap which refers to those of the patients that lie above the uppermost δS(QT) of H;

the latter from now on will be called $\delta S(\mathrm{QT})_{max,H}$. Thus, the limits of the patients we are currently interested in, do not extend from $\delta S(\mathrm{QT})_{min,\xi}$ to $\delta S(\mathrm{QT})_{max,\xi}$, since they must exceed $\delta S(\mathrm{QT})_{max,H}$, i.e.,

$$\delta S(QT) > \delta S(QT)_{max,H}. \tag{9.7}$$

The curve which corresponds to the one of the patients that has $\delta S(\mathrm{QT})$ lying just above the $\delta S(QT)_{max,H}$ corresponds to a value, which will be hereafter labeled $\delta S(\mathrm{QT})_{min',\xi}$ (e.g. see fig.3 of Ref. [63]). Thus, if we apply to each group ξ of patients the condition

$$\delta S(QT)_{min',\xi} \leq \delta S(QT) \leq \delta S(QT)_{max,\xi} \tag{9.8}$$

we are left only with those of the patients of the group ξ that actually overlap with SD.

We now recall that the measures λ, ρ, ν altogether, which are in fact ratios of δS values, enable the discrimination of the *vast* majority of SD from all the others (i.e., heart disease patients and H), while the $\delta S(\mathrm{QT})$ values themselves efficiently distinguish, as mentioned (see Fig. 9.7), *all* SD from H. This motivates us to investigate whether a proper combination of these two facts can serve our purpose, which refers to the identification of all SD among the other individuals (heart disease patients and H). Thus, we now compare the quantities $\lambda, \rho, \nu, \delta S(\mathrm{QT})$ altogether of each SD to the corresponding parameters of only those among the patients that happen to have $\delta S(\mathrm{QT})$ values exceeding the corresponding values of H, i.e., obey the condition (9.7), or preferably the more accurate condition (9.8).

Such a comparison reveals that some of the 17 parameters of λ, ρ, ν, $\delta S(\mathrm{QT})$, in all SD, lie outside the limits of these patients (cf. the same happens, of course, if we compare each SD to the limits of H). These results point to the conclusion that all 24 SD are distinguished from the patients (and H). The same conclusion is drawn if we consider instead, the 17 parameters λ, λ_{shuf}, ρ, $\delta S(\mathrm{QT})$.

We emphasize, however, that the study of the estimation errors (see § 9.2.7 and Section 9.3; see also the Appendix of Ref. [68]) reveals that:

The confidence level for the distinction of all SD from the patients becomes appreciably larger if we combine all the measures λ, λ_{shuf}, ρ ρ_{shuf}, ν (of all intervals) with the condition (9.8) applied to both $\delta S(\mathrm{QT})$ and $\delta S_{shuf}(\mathrm{QT})$ (i.e., in reality, we then consider the limits of those patients whom *both* $\delta S(\mathrm{QT})$ and $\delta S_{shuf}(\mathrm{QT})$ values are larger than those in H which are shown in Fig. 9.6).

A compilation of the limits of each of the complexity measures λ, ρ,λ_{shuf}, ρ_{shuf}, ν along with those of $\overline{\delta S}_{3-4}(QT)$ and $\overline{\delta S}_{3-4,shuf}(QT)$ in healthy humans (H) and in four groups (MIT, MSV, EST, MST) of heart disease patients is given in Table 9.5.

Table 9.5 Compilation of the limits of each of the complexity measures λ, ρ, λ_{shuf}, ρ_{shuf}, ν along with those of $\overline{\delta S}_{3-4}(QT)$ and $\overline{\delta S}_{3-4,shuf}(QT)$ in healthy humans (H) and in four groups (MIT, MSV, EST, MST) of heart disease patients. In parenthesis we put the limits which change when considering only the patients who have $\overline{\delta S}_{3-4}(QT)$ values larger than those in H, see § 9.2.4. The modified estimation errors, discussed in § 9.2.7, of the various parameters investigated are also shown. For the sake of brevity, the subscript "*sh*" stands for "*shuf*".

Parameter	H		MIT		MSV		EST		MST		$\varepsilon_m(\%)$
	min	max	min	max	min	max	min	max	min	max	
$\lambda_s(RR)$	1.43	2.00	0.80	1.96	0.85	1.22	0.79(0.94)	2.33	1.01	1.72(1.42)	11.66
$\lambda_L(RR)$	0.99	2.69	0.17	1.74	0.16	1.87	0.48(0.61)	6.66	0.45	3.75(2.68)	14.62
$\lambda_s(QRS)$	1.16	1.29	0.99	1.63	1.09	1.36	0.99	1.48	1.20	1.30(1.28)	10.53
$\lambda_L(QRS)$	0.48	0.61	0.46	0.71	0.47	1.06	0.42	1.63(0.90)	0.58	0.71(0.70)	11.19
$\lambda_s(QT)$	1.16	1.41	0.99	1.77	1.10	1.32	1.03(1.09)	1.71(1.36)	1.18	1.38	32.92
$\lambda_L(QT)$	0.50	1.11	0.33	0.96	0.50	0.74	0.43	2.82(1.73)	0.67	1.43(1.36)	41.37
$\rho_s(QRS)$	0.18	1.85	0.21	2.04	0.24	2.81	0.03	1.54	0.17	0.99(0.96)	18.23
$\rho_L(QRS)$	0.40	7.10	0.09	3.45	0.38	1.85	0.13	2.86(2.61)	0.51	2.62(1.25)	18.93
$\rho_s(QT)$	0.67	5.57	0.45	5.96	0.87	6.76	0.15	10.04(4.63)	0.53	4.98(1.97)	53.56
$\rho_L(QT)$	1.79	10.04	0.48	11.03	0.29	5.35	0.51	8.93(5.12)	1.11	8.70(2.07)	50.92
$\nu_s(RR)$ [a)]	1.10	2.27	0.86	1.64	0.84	1.94	1.01	11.11	1.76(2.30)	11.65	13.47
$\nu_L(RR)$ [a)]	0.44	0.77	0.59	2.48	0.51	2.75	0.31	1.90	0.44(1.93)	3.13	12.73
$\nu_s(QRS)$ [a)]	0.88	1.07	0.92	1.23	0.95	1.18	0.92(0.93)	1.25(1.19)	0.95	1.17	10.97
$\nu_L(QRS)$ [a)]	0.88	1.15	0.86	1.38	0.76	1.25	0.67(0.78)	1.25	0.83(0.97)	1.04	11.33
$\nu_s(QT)$ [a)]	0.91	1.46	0.95	1.20	0.97	1.58	0.96	3.04(1.82)	1.17	4.14	36.96
$\nu_L(QT)$ [a)]	0.65	1.07	0.74	1.38	0.76	1.31	0.50	1.75	0.59(0.95)	2.22	37.33
$\overline{\delta S}_{3-4}(QT) \times 10^3$	0.23	0.56	0.79	3.71	0.45(0.61)	4.59	0.20(0.56)	5.75	0.22(0.63)	1.33	28.51
$\lambda_{s,sh}(RR)$	1.04	1.27	0.92	1.34	0.96(1.05)	1.24	1.00	1.26	1.11(1.16)	1.21	11.00
$\lambda_{L,sh}(RR)$	0.48	0.57	0.37	0.92	0.45	0.54	0.43(0.46)	0.58	0.50(0.51)	0.56	10.86
$\lambda_{s,sh}(QRS)$	1.10	1.44	1.13	1.46	1.15	1.37	1.10(1.11)	1.47(1.43)	1.10	1.43	11.34
$\lambda_{L,sh}(QRS)$	0.46	0.73	0.47	0.75	0.49	0.80	0.51	0.96(0.77)	0.50(0.51)	0.69	12.27
$\lambda_{s,sh}(QT)$	1.12	1.32	0.89	1.26	0.85	1.23	1.10	1.56	1.17	1.28(1.24)	32.46
$\lambda_{L,sh}(QT)$	0.49	0.70	0.37	0.57	0.43	0.60	0.49	0.70	0.52	0.57	35.29
$\rho_{s,sh}(QRS)$	0.39	3.02	0.29	2.35	0.27	2.54	0.08	2.47(1.78)	1.07(1.75)	3.34	17.71
$\rho_{L,sh}(QRS)$	0.30	3.21	0.20	4.22	0.27	1.64	0.06	2.52(1.67)	0.97(1.48)	3.66	18.29
$\rho_{s,sh}(QT)$	1.25	9.63	0.46	7.01	0.75	6.13	0.57	10.50(6.71)	4.31	9.95(8.54)	53.11
$\rho_{L,sh}(QT)$	1.34	7.30	0.56	13.04	0.62	5.07	0.54	6.81(3.26)	1.80	7.03(3.62)	50.69
$\overline{\delta S}_{3-4,sh}(QT) \times 10^3$	0.27	0.66	0.79	3.84	0.46(0.67)	4.57	0.32(0.63)	9.07	0.31(1.57)	3.12	28.50

a)The values of these quantities do not fully coincide with those given in Ref. [66] for the reasons discussed in § 9.2.7.

Table 9.6 The number of SD and patients that can be distinguished from H when using λ_κ(RR) or $\lambda_{\kappa,shuf}$(RR) *alone*.

Group	Total number of individuals	λ_κ(RR)	$\lambda_{\kappa,shuf}$(RR)	λ_κ(RR) and $\lambda_{\kappa,shuf}$(RR)
SD	24	23	10	24
MIT	15	14	6	14
MSV	13	13	2	13
EST	33	29	8	29
MST	6	5	0	5

We now comment on two points.

First, since it is known that heart rate variability depends strongly on age, it is highly recommended that when comparing values of the aforementioned complexity measures, the corresponding limits should be taken from subjects (heart disease patients and H) of comparable age [66].

Second, we now focus on the importance of the sequential order of Q_m on the aforementioned complexity measures. We prefer to deal with the results related to the RR intervals since it is known that the healthy heart beats irregularly and that the RR intervals fluctuate widely, following complicated patterns [9]. Let us investigate, for example, the possibility of using λ_κ(RR) alone to distinguish the SD as well as the four groups of patients from H, i.e., examine whether the λ_κ(RR) values of each individual violate one (at least) of the relevant *H-limits*.

The results show (see Table 9.6) that the vast majority of SD and of each group of patients is well distinguished from H by means of λ_κ(RR) *alone*.

The situation drastically changes, however, if we use, instead of λ_κ(RR), the $\lambda_{\kappa,shuf}$ values (see the tables V to VII in Ref. [63]): only the minority of SD and of each group of patients can be differentiated from H. Since the calculation of the λ_κ(RR) values takes into account the sequential order of Q_m, while the $\lambda_{\kappa,shuf}$(RR) values do not, this points to the following conclusion:

It is the *sequential* order of beats that contains the primary information which enables the distinction between the SD and heart disease patients, on the one hand, and the H, on the other.

This might explain why procedures based on the entropy in natural time (which is dynamic entropy, affected by the sequential order [67]) – and hence consider the complexity measures mentioned in § 9.2.1 – can achieve such a distinction, while static entropy (e.g., Shannon entropy, see Ref. [67]) cannot.

9.2.5 Distinction of heart disease patients from H

This distinction can be made by identifying as heart disease patients the individuals whom one or more of the parameters associated with λ, ρ, ν (of RR, QRS, QT) and $\delta S(QT)$ violate the *H-limits provided* that the distinction of the SD has been *preceded* by the procedure described above in § 9.2.4.

Furthermore, comparing each of the tables in Ref. [63] that present the aforementioned parameters for each group of heart disease patients to (the H in) Table 9.2, we also find that:

In *all* heart disease patients, at least one of their four λ parameters associated with RR and QRS, i.e., $\lambda_s(RR)$, $\lambda_L(RR)$, $\lambda_s(QRS)$ and $\lambda_L(QRS)$, violates one of the corresponding *H-limits*, thus allowing again a distinction between patients and H. In other words, only four parameters are needed to distinguish heart disease patients from H.

A further inspection reveals that among the limits of these four λ parameters most of the heart disease patients violate the ones of $\lambda_s(RR)$ and/or $\lambda_L(RR)$.

Thus, in a future population consisting of all three categories SD, heart disease patients and H, in order to separate the last two, we may work as follows. By considering the limits given in Table 9.5, we first apply the procedure to identify the SD (as described in § 9.2.4) among the other individuals, thus only heart disease patients and H remain. It seems then that, in the latter population, the λ parameters of the RR and QRS can efficiently distinguish heart disease patients from H (this can be further strengthened by the additional use of the corresponding ν parameters, which differentiate most of the heart disease patients – but *not* all of them – from the H). In other words, any (explicit) information on the QT may not be prerequisite to distinguish between heart disease patients and H. This is consistent with the aforementioned (§ 9.1.1) clinical observations that the prolongation of the QT (due to the lengthening of the ST interval) is mainly a characteristic of the SD.

9.2.6 Complementarity of the complexity measures for identifying sudden cardiac death individuals (SD)

We first discuss the complementarity of the two procedures described above in § 9.1.3 and § 9.2.2 for the distinction of the (otherwise healthy) SD from H, i.e., *if* the population under investigation does *not* include heart disease patients.

Recall that in § 9.1.3 entropy fluctuations – deduced from the original and the "shuffled" time series – on *fixed* time-scales have been employed, while in § 9.2.2 entropy fluctuations on *different* time-scales have been considered.

This complementarity holds in the following sense: if in the frame of the one procedure an ambiguity emerges in the distinction between SD and H, the other procedure gives a clear answer.

We now study, as an example, the following two procedures: i.e., the one that uses δS(QT) (see § 9.1.3) and the other which combines the measures λ, ρ (see § 9.2.2). The $\overline{\delta S}_{3-4}$(QT) values of SD and H given in the last column of Table 9.2 are classified into two classes: the larger values correspond to SD, and the lower ones correspond to H (see also Figs. 9.7 and 9.12). Let us focus on the two lowermost SD values and the uppermost H value. The former two correspond to sel33 and sel34 ($\overline{\delta S}_{3-4}(\text{QT}) = 0.00076$ and 0.00069, respectively) and the latter one to sel16795 ($\overline{\delta S}_{3-4}(\text{QT}) = 0.00056$). In view of their $\overline{\delta S}_{3-4}$(QT) values proximity, one may wonder whether these two SD could be confused with H. This ambiguity can be resolved in the light of the other procedure (i.e., λ, ρ), as follows. Table 9.2 reveals that sel33 markedly violates both the H_{min}*-limit* for λ_s(QRS) and H_{min} for λ_s(RR) (the latter can be visualized in Fig. 9.13). As for sel34, the H_{max}*-limit* of λ_L(QRS) is strongly violated. We now turn to an alternative example, i.e., sel47, which, by means of the method using the complexity measures λ, ρ (of the RR and QRS intervals, see § 9.2.2) could be confused with H, because a deviation of only around 12% from the H_{min}*-limit* of $\min_H[\rho_s(QRS)] = 0.18$ is noticed. This ambiguity can be resolved by means of the procedure using δS(QT) (§ 9.1.3) as follows: sel47 has $\overline{\delta S}_{3-4}(\text{QT}) = 0.0029$, which exceeds significantly, i.e., by a factor 5, the corresponding value of sel16795, who has the largest $\overline{\delta S}_{3-4}(\text{QT}) = 0.00056$ value among the H.

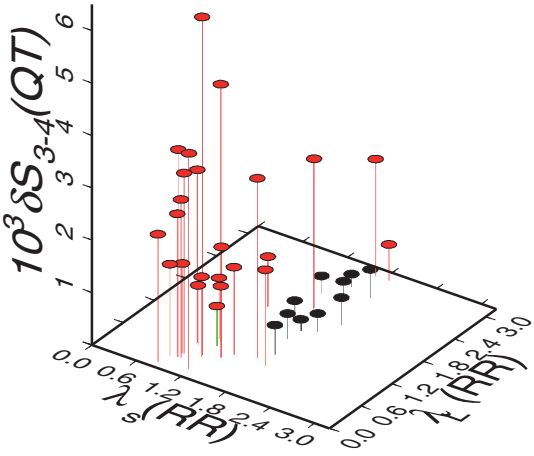

Fig. 9.13 The $\overline{\delta S}_{3-4}$(QT) values along with those of λ_s(RR) and λ_L(RR) for SD (red) and H (black). The individual sel33 is marked with a green column. Taken from Ref. [68].

We now turn to the investigation (for details see Ref. [63]) of the complementarity of the *four* quantities λ, ρ, ν and $\delta S(QT)$ on differentiating *all* SD from the others (i.e., heart disease patients and H). This can be judged from an inspection of Table 9.7, which contains the results to distinguish the SD among 101 individuals, for all possible combinations, upon considering only *three* of these quantities (i.e., see the cases in Table 9.7 except of the upper two where all four quantities are used). For example, the combination λ, ρ, ν cannot differentiate four SD (i.e., sel30, sel32, sel34, sel37) from the heart disease patients. As a

Table 9.7 Results of the distinction of 24 SD among 101 individuals upon using combinations of the measures λ, ρ, ν along with $\overline{\delta S}_{3-4}(QT)$. Taken from Ref. [63]

Measures combined[a)]	The non-differentiated SD[b)]	Number of SD distinguished
λ, ρ, ν and relation (9.8)	**None**	24 **(all)**
λ, ρ, ν and relation (9.7)	**One:** sel35(MIT)	23
λ, ρ, ν	**Four:** sel30(EST), sel32(EST), sel34(EST), sel37(EST)	20
λ, ρ and relation (9.8)	**Four:** sel30(MSV), sel41(MIT), sel46(MIT), sel49(MSV)	20
ρ, ν and relation (9.8)	**Three:** sel33(MSV,EST), sel45(MIT,MSV), sel46(MSV,EST)	21
λ, ν and relation (9.8)	**Seven:** sel36(MIT,EST), sel38(MIT), sel41(MSV), sel42(EST), sel47(EST), sel51(EST), sel17152(MSV,EST)	17
λ, ρ, ν of RR and QRS only	**Twelve:** sel30(EST), sel32(EST), sel34(EST), sel35(MIT,MSV), sel37(EST), sel38(MIT), sel40(EST), sel43(EST), sel45(MSV), sel47(EST), sel50(MIT), sel51(EST)	12

a) In all cases the data of the five heart disease patients sel230, sel231, sele0612, sele0704, sele0136 have been excluded (see § 9.2.4).
b) In parenthesis we mark the group(s) of heart disease patients in which the corresponding SD is mislocated.

second example, the combination ρ, ν and $\delta S(QT)$ cannot identify three SD (i.e., sel33, sel45, sel46), who are *different* from the four that could *not* be discriminated by the former combination λ, ρ, ν. By the same token, we find that each of the remaining combinations fails to identify certain SD, who can be distinguished by another combination(s).

Therefore, we conclude that each of the four quantities λ, ρ, ν, $\delta S(QT)$ seems to *complement* the others in identifying all SD (note that the same conclusion is drawn if we alternatively use the four quantities λ, λ_{shuf}, ρ and δS(QT); see table XIII of Ref. [63]).

In general, measures that employ entropy fluctuations of the original and shuffled time series on fixed time-scales, seem to complement those that take into account entropy fluctuations on different time-scales.

This might be understood in the context that each of these quantities, as already mentioned, presumably captures certain "elements" of heart dynamics only. As for the *necessity* of using all these quantities, it might stem from the following fact. The database we used, consists of SD individuals in which different physiological processes might have led to sudden cardiac death. The selection of such a *heterogeneous* database was intentionally made, because it was our aim to find, if possible, a general procedure for identifying SD. If a study of "homogeneous" SD databases (in the sense that the same physiological processes preceded the sudden cardiac death) is made, it may happen that a smaller number

of parameters are necessary to distinguish *all* SD. Until the completion of such studies, however, it is recommended to use *all* the parameters associated with the aforementioned quantities, as described in Ref. [68].

9.2.7 The estimation errors in the procedure for identifying SD

Beyond the error introduced by the use of an automatic threshold detector for the allocation of the corresponding intervals which is largest for the QT and smallest for the RR intervals, the following two sources of errors must be considered [67, 68]: First, an estimation error emerges when analyzing – instead of the original time series of length $l \approx 10^3$ heartbeats – smaller lengths l' (e.g., see Table 9.3), which, however, still significantly exceed the time-window lengths used, for example $l' \approx 2 \times 10^2$ (obviously the errors associated with the measures in the short-range, s, are smaller from those corresponding to the longer range, L, because for the latter range the l/l' values – due to the restricted length of the records available – are small, thus not allowing more reliable statistics). Second, a source of (statistical) error in the results emerges when considering the ratio(s) $\delta S_{shuf}/\delta S$ (i.e., when dealing with ν and λ_{shuf}) instead of δS itself. While δS may be considered to have a *unique* value for a (given) original Q_m time series, the value of δS_{shuf} depends on the randomly shuffled Q_m series each time selected (note that such differences are well known [23] when dealing with randomized series of *finite* length). This is why the ν values given in Ref. [67] for SD and H do not fully coincide with those tabulated in Ref. [68]. To account roughly for the extent of this statistical error, we averaged here the δS_{shuf} values calculated over a number (e.g. 20) of randomly shuffled Q_m-series generated from the *same* original series and the corresponding standard deviation was estimated.

The final results of the above sources, could be summarized as follows [68]: The (percentage) estimation error was found to be on the average ≈10% for the complexity measures λ,λ_{shuf}, ρ, ρ_{shuf}, ν associated with the RR and QRS intervals. Furthermore, since the error in the δS(QT) may reach 20%, the estimation error in those of the complexity measures that involve δS(QT) may be as high as ≈30%. Upon considering such error-levels, hereafter called "*plausible estimation errors*" ε_p, a study of each of the methods for the distinction of SD was made. The study was repeated by assuming larger (percentage) estimation errors, hereafter labeled "*modified estimation errors*" ε_m, calculated for each parameter from

$$\varepsilon_m = \varepsilon_p \left(1 + \frac{H_{max} - H_{min}}{H_{max} + H_{min}} \right), \tag{9.9}$$

see the last column in Table 9.5. Both studies led, more or less, to the same results, e.g., those obtained when using ε_m, which are tabulated in columns 5–7 in Table 9.8. The calculation, in each study, was made as follows. Each parameter was assumed to be equal to its value (initially estimated from the original time series available) multiplied by a number randomly selected in the range $1 \pm \varepsilon_p$ or $1 \pm \varepsilon_m$, respectively) and then each of the methods for the distinction of SD was applied. This application was repeated, for each method, 10^3 times via Monte Carlo.

Table 9.8 The confidence levels to distinguish SD from either H or heart disease patients when considering the estimation errors ε_m of Eq. (9.9) discussed in § 9.2.7 and given in Table 9.5. Taken from Ref. [68].

Method employed				Confidence levels to distinguish SD						
				Using the limits from the data analyzed			Using broader limits[c)]			
Aim	Measures	Type of intervals	No. of parameters	All SD %	All but one SD %	All but two SD[d)] %	All SD %	All but one SD %	All but two SD %	All but five SD[d)] %
Distinction of SD from H	λ, ρ	RR, QRS, QT	10	>99	>99	>99	88	99	>99	>99
	λ, ρ	RR, QRS	4	63	95	>99	8	43	90	>99
	λ, λ_{shuf}	RR	4	49	90	99	1	11	36	97
	ν	RR,QRS	4	32	74	96	<0.5	1	8	60
	$\delta S_{3-4}(QT)$	QT	1	59	93	>99	11	39	77	>99
	$\lambda, \rho, \lambda_{sh}, \rho_{sh}, \nu, \delta S_{3-4}(QT), \delta S_{sh,3-4}(QT)$	RR, QRS, QT	28	>99	>99	>99	>99	> 99	>99	>99
Distinction of SD from heart disease patients	$\lambda, \rho, \nu, \delta S_{3-4}(QT)$[a)]	RR, QRS, QT	17	51	83	95	<0.1	<0.1	<0.1	1
	$\lambda, \rho, \lambda_{sh}, \delta S_{3-4}(QT)$[a)]	RR, QRS, QT	17	62	91	98	<0.1	<0.1	<0.1	1
	$\lambda, \rho, \lambda_{sh}, \rho_{sh}, \nu, \delta S_{3-4}(QT), \delta S_{sh,3-4}(QT)$[b)]	RR, QRS, QT	28	95	>99	>99	16	41	68	98

a) Considering the limits of those patients that have $\delta S_{3-4}(QT)$ larger than those in H.
b) Considering the limits of those patients that have *both* $\delta S_{3-4}(QT)$ and $\delta S_{sh,3-4}(QT)$ larger than those in H.
c) By amounts ε_m of Eq. (9.9) discussed in § 9.2.7 and given in Table 9.5.
d) When stating, e.g., "All but one", it means that when allowing *at the most*, one SD – out of 24 – to be misinterpreted as being H or heart disease patient, respectively.

The extent to which these conclusions hold, was also investigated in the following *extreme* case: the limits of the parameters of H (and patients), which are automatically adjusted for each "random" selection of the values described above, have been assumed to *additionally* relax by (extra) amounts equal to ε_p or ε_m. Such a "relaxation" faces the *extreme* possibility that the populations of H and heart disease patients analyzed here are not considered large enough to allow a precise determination of their limits, and hence future increased populations' studies could somehow broaden these limits by *extra* amounts as large as ε_p or ε_m. The corresponding confidence levels to distinguish SD from either H or heart disease patients can be found in the last four columns of Table 9.8.

9.3 Summarizing the conclusions for identifying sudden cardiac death individuals (SD) upon considering the error levels

As already mentioned in § 9.1.1, sudden cardiac death may occur *even if* the ECG looks similar to that of truly healthy humans. In other words, we are interested here in the distinction of the (otherwise healthy) SD from H, i.e., *if* the population under investigation does *not* include heart disease patients. To distinguish such cases, i.e., when we consider a set consisting *only* of two groups of ECG, namely H and SD, the conclusions drawn from the procedures developed in § 9.1.3 and § 9.2.2 above, are summarized below in § 9.3.1 and the relevant confidence levels are compiled in Table 9.8 under the Aim "Distinction of SD from H". As for the procedures developed to identify SD in a population that includes H as well as heart disease patients (§ 9.2.4) that led to the limits compiled in Table 9.5, the conclusions are summarized in § 9.3.2 and the corresponding confidence levels are given in Table 9.8 against the Aim "Distinction of SD from heart disease patients".

9.3.1 Summary of the conclusions for distinguishing SD from H

Among the four methods suggested (i.e., two in § 9.1.3 and two in § 9.2.2), the one that uses the measures λ, ρ (associated, however, with *all* three types of intervals, i.e., 10 parameters in total, see first row in Table 9.8) seems to be robust [68] in the following sense:

(i) When assuming the error-levels (see § 9.2.7) deduced from the data analyzed here (the relevant results are inserted in Table 9.8 under the heading "Using the limits from the data analyzed"):

> The use of λ, ρ related to *all* intervals, thus 10 parameters in total, allows the distinction of *all* SD from H with a confidence level above 99%.

The confidence level decreases to 63%, 49%, 32% and 59% when using either four parameters or one parameter only as follows: first: λ_κ(RR) and ρ_κ(QRS); second: λ_κ(RR) and $\lambda_{\kappa,shuf}$(RR); third: ν_κ(RR) and ν_κ(QRS); fourth: $\overline{\delta S}_{3-4}$(QT), respectively.

(ii) If we investigate the extreme case of the additional "relaxation" of the *H-limits* mentioned in § 9.2.7 (the relevant results in Table 9.8 are under the heading "Using broader limits"), the capability for the distinction of *all* SD still remains with the following results:

In the case of using solely λ, ρ for all intervals, the confidence level in distinguishing *all* SD is 88%. It becomes *appreciably higher*, i.e., larger than 99%, if we use the quantities λ, ρ, λ_{shuf}, ρ_{shuf}, ν, $\overline{\delta S}_{3-4}(QT)$, $\overline{\delta S}_{3-4,shuf}(QT)$ *altogether*.

When using, however, four parameters only in the first three combinations mentioned above, the confidence level decreases to 90%, 36% and 8%, respectively (and to 77% when using $\overline{\delta S}_{3-4}$(QT)), even when allowing two at the most SD – out of 24 – to be misinterpreted as being H.

9.3.2 Summary of the conclusions for identifying SD among individuals that also include heart disease patients and H

The corresponding conclusions related to the distinction of SD from heart disease patients can be drawn on the basis of the values given in the lower part of Table 9.8.

In summary, the study of the estimation errors reveals [68] that *if* the limits of the parameters that have been deduced from the ECG data analyzed here will *not* be broadened by future investigations:

We can satisfactorily distinguish the *totality* of SD from H as well as discriminate the totality of SD from heart disease patients, upon employing the quantities λ, λ_{shuf}, ρ, ρ_{shuf}, ν,$\overline{\delta S}_{3-4}$(QT), $\overline{\delta S}_{3-4,shuf}$(QT) *altogether*, i.e., the sixth and the last method in Table 9.8, respectively.

These quantities also allow the distinction of the *totality* of SD from H (as well as distinguish the *vast majority* of SD from the heart disease patients) *even if* their limits will be eventually broadened (by ε_m of Eq. (9.9), see § 9.2.7).

Concerning the number of parameters required to achieve the desired distinction [68]: In reality, only twelve *independent* quantities, (i.e., the six: $\delta S_\kappa(\tau)$ and the six $\delta S_{\kappa,shuf}(\tau)$, where $\kappa = s, L$ and $\tau =$ RR, QRS, QT) are extracted from the experimental data. Thus, for example, beyond $\overline{\delta S}_{3-4}(QT)$ *or* $\overline{\delta S}_{3-4,shuf}(QT)$, eleven additional parameters (out of 26) of the ratios: λ, λ_{shuf}, ρ, ρ_{shuf}, ν are in principle required to be used for the distinction. These twelve quantities, however, should *not* be fortuitously selected, but the following points must be carefully considered: (i) priority should be given to the eight parameters associated with λ values and λ_{shuf} (or ν) values of RR and QRS, (ii) using, at least, one ρ-parameter (involving $\overline{\delta S}_{3-4}(QT)$ or $\overline{\delta S}_{3-4,shuf}(QT)$), and (iii) examining whether the totality of the parameters used can actually reproduce the aforementioned twelve δS values determined directly from the data. However, in order to avoid the difficulty arising from the completeness (or not) of the aforementioned selection, at the present stage (i.e., until an

appreciably larger number of H and heart disease patients will be analyzed to allow a better precision in the determination of the corresponding limits, see § 9.2.7), it is recommended to use – instead of twelve – *all* the 28 parameters associated with the quantities λ, λ_{shuf}, ρ, ρ_{shuf}, ν, $\overline{\delta S}_{3-4}(QT)$ and $\overline{\delta S}_{3-4,shuf}(QT)$.

9.4 The change ΔS of the entropy in natural time under time reversal: identifying the sudden cardiac death risk and specifying its occurrence time

9.4.1 Specifying the occurrence time of the impending cardiac arrest by means of ΔS

Here, we make use of the Definition 3.2 of ΔS (see Eq. (3.64)) and the points developed in § 3.5.1.

In particular, a window of length l is sliding, each time by one pulse, through the whole time series. The entropies S and S_-, and therefrom their difference ΔS_l, are calculated each time. Thus, we form a new time series consisting of successive ΔS_l values.

We will show and that the determination of the occurrence time of the impending cardiac arrest can be obtained [69] from the time evolution of ΔS_l deduced from the RR time series.

9.4.1.1 The ECG data analyzed in natural time

These are 159 long-lasting (from several hours to around 24 h) ECG recordings, which come from databases [14], containing: (i) 72 healthy subjects, (ii) 44 patients with congestive heart failure (CHF) (iii) 25 subjects with atrial fibrillation (AF) and (iv) 18 individuals suffered sudden cardiac death. In particular (see Ref. [65]), these data come from the following databases [14]: (i) the MIT-BIH Normal Sinus Rhythm Database (nsrdb) containing 18 H digitized with frequency $f_{exp} = 128$ Hz, (ii) the Normal Sinus Rhythm RR Interval Database (nsr2db) containing 54 H, $f_{exp} = 128$ Hz (iii) the Congestive Heart Failure RR Interval Database (chf2db) containing 29 subjects with congestive heart failure, $f_{exp} = 128$ Hz, (iv) the BIDMC Congestive Heart Failure Database (chfdb) with 15 subjects with severe congestive heart failure, $f_{exp} = 250$ Hz (v) the MIT-BIH Atrial Fibrillation Database (afdb) with 25 subjects with atrial fibrillation (AF) mostly paroxysmal, $f_{exp} = 250$ Hz and (vi) the Sudden Cardiac Death Holter Database (sddb), $f_{exp} = 250$ Hz. The latter contains 24 SD among which 12 had ECG with audited annotations. Here, beyond these 12 individuals, we studied six more (i.e., "33", "37", "44", "47", "48", "50") whose ECG could be analyzed with confidence. Thus, we consider 18 (out of 24) SD individuals of the sddb.

The results presented in this Section refer to the RR intervals (see Fig. 2.2), i.e., $Q_m = \mathrm{RR}_m$. For reasons that will be explained later, the study will be extended (in all these 159 individuals except the 25 AF for which NN annotations were not available) to the so-called NN intervals, i.e., $Q_m = \mathrm{NN}_m$. These are intervals obtained from ECG annotation files by using the option [41] "-c -PN pN", which yields only intervals between consecutive *normal* beats, while intervals between pairs of *normal* beats surrounding an ectopic beat are discarded. In both the RR and NN time series, in order to exclude "outliers" from the records, the detection algorithm proposed in Ref. [21] has been applied, i.e., for each set of five contiguous intervals, if the local mean, excluding the central interval, is larger than twice the central interval then this interval is excluded from further analysis. In Fig. 9.15(a) one H out of 72, i.e., the one labeled 16539, has been discarded because the resulting $\sigma[\Delta S_3]$(NN) value was unusually high compared to that in other H of nsrdb (see table 2 of Ref. [65]). Furthermore, in Fig. 9.15(b), three H out of 72 (i.e., 16539, nsr024 and nsr044) have been also discarded since they have $\sigma[\Delta S_3]$(RR) value unusually higher than that in other H (see table 2 of Ref. [65]). For more details on the annotators used see Ref. [65].

Table 9.9 Results of the application of the complexity measure ΔS_l to the *RR* time series: the extrema $\max(\Delta S_{13})$ and $\min(\Delta S_{13})$ in SD along with the time of their occurrence, i.e., T_{max} and T_{min}, respectively. The latter time is measured from the time of the VF onset (except for "49", who paced with no VF). In the last column, the total duration of the record T_{total} measured from the time of the VF onset is also inserted. Taken from Ref. [65].

Individual	$\max(\Delta S_{13})$	$T_{\max}$(s)	$\min(\Delta S_{13})$	$T_{\min}$(s)	T_{total} (s)
30	0.0129	28,150.65	−0.0107	6,000.90	28,470.75
31	0.0182	1,497.47	−0.0174	1,492.78	49,341.89
32	0.0069	59,754.38	−0.0047	59,746.80	60,315.61
33	0.0168	3,021.60	−0.0237	11,212.63	17,176.40
34	0.0102	10,642.46	−0.0097	7,408.24	23,743.42
35	0.0214	22,674.56	−0.0220	7,872.32	86,398.19
36	0.0218	5,603.68	−0.0197	5,598.33	68,338.58
37	0.0355	5,361.32	−0.0569	5,370.84	5,470.82
41	0.0240	3,303.27	−0.0212	3,060.47	10,762.66
44	0.0146	7,993.19	−0.0123	34,421.23	70,723.33
45	0.0157	62,992.88	−0.0145	62,985.09	65,354.88
46	0.0184	13.38	−0.0166	5,244.22	13,304.91
47	0.0241	13,282.90	−0.0230	8,481.94	22,378.26
48	0.0146	8,921.66	−0.0150	8,930.64	8,978.57
49	0.0145	5,677.80	−0.0140	1,805.06	84,528.44
50	0.0353	1,349.73	−0.0347	4,349.58	42,339.39
51	0.0151	53,067.89	−0.0161	1,957.63	82,701.48
52	0.0293	2,552.97	−0.0252	2,567.82	9,158.85

9.4.1.2 Presentation of the ΔS_l results

In Fig. 9.14(a), we give as an example the time series of ΔS_{13} for one SD, i.e., the one labeled "30". In the horizontal axis the time is measured from the ventricular fibrillation (VF) onset. The time of the VF initiation for each SD (except for the individual "49", who

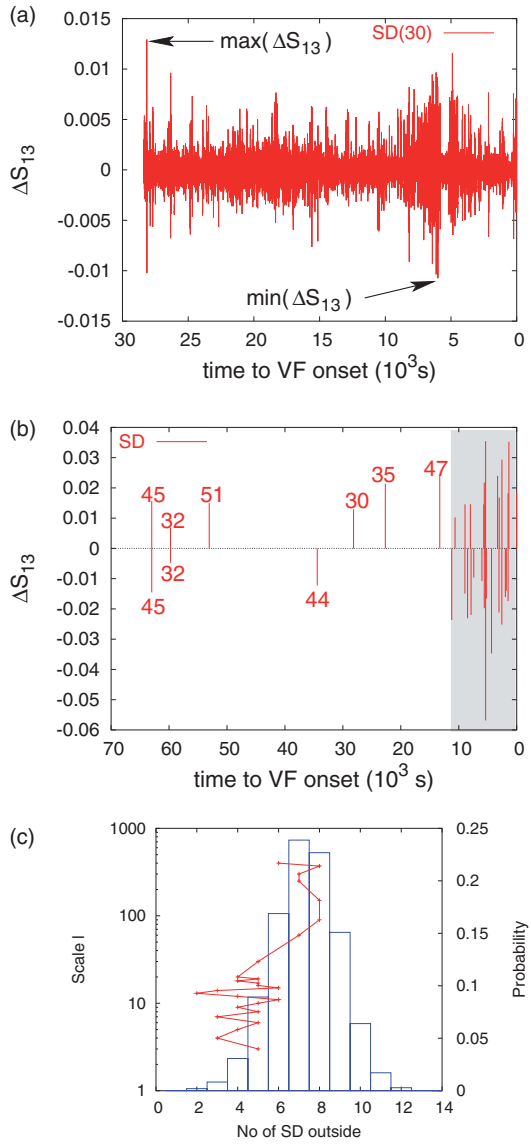

Fig. 9.14 Results from the analysis of the RR time series: (a) Plot of the quantity ΔS_{13} versus the time to the VF onset for one SD, i.e., "30". The quantities $\max[\Delta S_{13}]$ and $\min[\Delta S_{13}]$ are shown by arrows. (b) For each of the 18 SD (each bar corresponds to each individual), we plot the $\max[\Delta S_{13}]$ value – in the upper part (i.e., positive ΔS_{13} axis) – and the value $\min[\Delta S_{13}]$ – in the lower part (i.e., negative ΔS_{13} axis) – versus the time it appeared *before* the VF onset. The shaded part indicates the last 3 h *before* the VF onset. (c) The red curve shows the number of SD that violate *both* conditions $T_{\max} \leq 3$ h and $T_{\min} \leq 3$ h as a function of scale l. The probability achieving by chance the relevant number of SD is drawn by blue bars (right vertical scale). Reprinted with permission from Ref. [69]. Copyright (2007), American Institute of Physics.

paced with no VF) is given in the database used [14]. The VF initiation remains one of the leading immediate causes of sudden cardiac death [1]. The maximum and the minimum values of ΔS_{13} will be labeled $\max[\Delta S_{13}]$ and $\min[\Delta S_{13}]$, respectively. The time of their appearances are designated $T_{\max}$ and $T_{\min}$, respectively. An inspection of Fig. 9.14(a) in conjunction to Table 9.9, reveals that $T_{\max} \approx 28{,}150$ s and $T_{\min} \approx 6{,}000$ s (before the VF onset). The corresponding values for all the other SD studied, are also given in the same Table, which presents the extrema of ΔS_{13} along with the time of their appearance. These

values, which are depicted in Fig. 9.14(b), reveal that interestingly in the vast majority of SD (i.e., in all the 18 SD except the individuals "32" and "45", the latter having a history of ventricular ectopy) they are smaller than around 3 hours. In other words, *only* for two individuals (i.e., "32" and "45") out of eighteen, *both* $T_{\rm max}$ and $T_{\rm min}$ are larger than around 3 hours. The results for a variety of other length scales are summarized in Fig. 9.14(c), where we plot in red the number of SD that violate *both* conditions, i.e., $T_{\rm max} \leq 3$ h and $T_{\rm min} \leq 3$ h, at various scales. The probability having such a result by chance is also shown in the right vertical scale. This probability has been found by Monte Carlo calculation, in which the observation times for *both* extrema, i.e., $T_{\rm max}$ and $T_{\rm min}$, were assumed to be uniformly distributed within the total duration $T_{\rm total}$ of the record for each individual (see Table 9.9). We observe that for small scales ($l < 30$) the observed number of SD differs significantly from the one expected by chance. Especially, the probability to find by chance the result obtained at $l = 13$ is smaller than 0.2%.

In other words, an optimum length scale (i.e., $l = 13$ heartbeats) exists, at which the magnitude of ΔS_l (deduced from the RR time series, alone) maximizes (in 16 out of 18 cases) ≈ 3 hours at the most before the VF onset, thus signaling the imminent cardiac death risk.

Since many SD experience arrhythmia (consisting of one or more types including premature ventricular contractions (PVCs), AF and non-sustained tachycardia), it has been confirmed (through a direct inspection of the ECG) that the extreme values of ΔS_{13} in Fig. 9.14(b) mainly come from trains of occurrences of PVCs. We emphasize, however, that beyond the PVCs, the method of ΔS_l captures *additional* elements of cardiac dynamics that distinguish SD from other individuals as will be discussed in § 9.4.2.

9.4.2 Identifying the sudden cardiac death risk by means of complexity measures based on ΔS

We now make use of the points treated in § 3.5.1 and § 3.6.2. In particular, following § 3.5.1, we recall that when we form the new time series consisting of successive ΔS_l values, the standard deviation of these values is denoted by $\sigma[\Delta S_l]$. Upon shuffling the Q_m randomly (thus destroying any information hidden in the *ordering* of the events), the ΔS_l values turn to a sequence of different values labeled $\Delta S_l^{\rm shuf}$ whose standard deviation is designated by $\sigma[\Delta S_l^{\rm shuf}]$ (its theoretical estimation was given in § 3.5.2). The complexity measure $N_l \equiv \sigma[\Delta S_l^{\rm shuf}]/\sigma[\Delta S_l]$ (see Eq. (3.83)), which quantifies the extent to which the ordering of the heartbeats contributes to the ΔS_l values (being unity for a *random* process), is also computed.

In Fig. 9.15(a), we plot the quantities N_3(NN) versus $\sigma[\Delta S_7]$(NN) deduced from the analysis of the NN time series of all individuals except of the 25 AF (since for the latter, relevant NN annotations were not available).

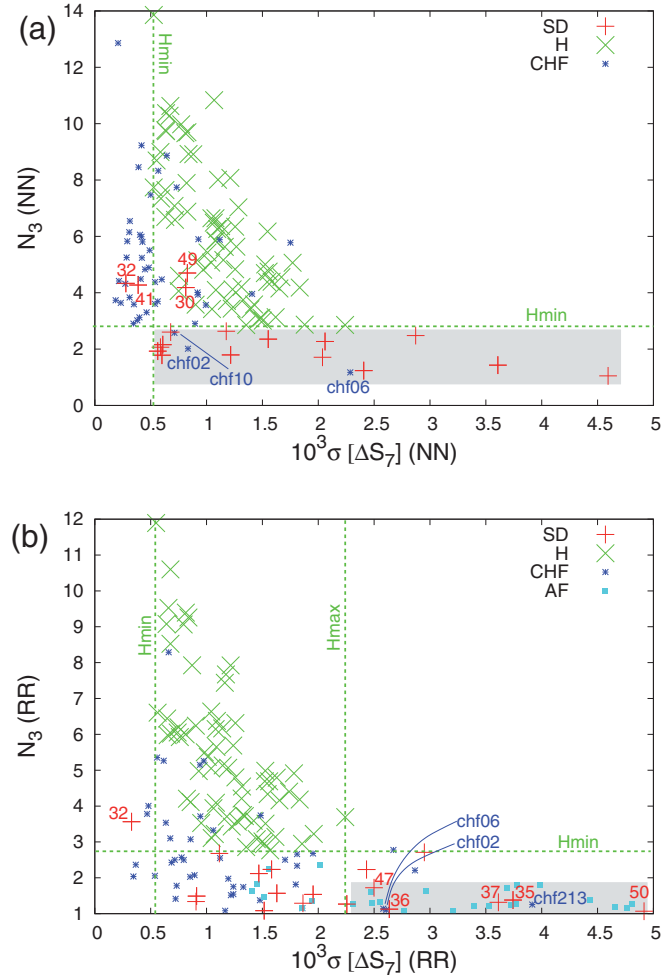

Fig. 9.15 The quantity N_3 versus $\sigma[\Delta S_7]$ for (a) the NN and (b) the RR time series. The green horizontal line corresponds to the minimum N_3 value computed in H. Reprinted with permission from Ref. [69]. Copyright (2007), American Institute of Physics.

Thus, when using the NN time series alone, an inspection of Fig. 9.15(a) reveals the major importance of the measure N_3(NN) in two respects.

First, the vast majority of SD (i.e., 14 out of 18, lying in the shaded region) exhibit N_3(NN) values that are *smaller* than the minimum N_3(NN) value computed among the H which is labeled $H_{\min}$ and marked with a horizontal green line in Fig. 9.15(a).

Second, the vast majority of CHF have N_3(NN) values *larger* than $H_{\min}$, thus allowing in principle a distinction between CHF and SD.

In Fig. 9.15(b), we plot N_3(RR) versus $\sigma[\Delta S_7]$(RR) deduced from the RR time series. This figure shows that the distinction between CHF and SD achieved in Fig. 9.15(a) is now lost. This is understood in the context that frequent PVCs influence the RR time series (but *not* the NN) of *both* CHF and SD.

Thus, when using the RR time series alone, a closer inspection of Fig. 9.15(b) reveals two important points:

First, almost *all* SD (i.e., except "32") exhibit N_3(RR) values that are smaller (hence high complexity breaks down) than the minimum value $H_{\min}$ computed in H, thus emphasizing again the importance of the scale $l = 3$.

Second, the shaded region that contains the vast majority of AF (18 out of 25) lies to the right of the maximum value of $\sigma[\Delta S_7]$(RR) observed in H, labeled $H_{\max}$ (see the rightmost vertical green line). Four out of the five SD (i.e., except "47") located in this region, suffered from atrial fibrillation, thus this shaded region seems to separate AF from the others.

Thus, in short, the aforementioned method *not only* identifies the sudden cardiac death risk *but also* provides a distinction of congestive heart failure patients from SD when NN annotations are available.

9.4.3 Summary of the findings based on ΔS and their tentative explanation

In order to understand the physical origin of the findings in § 9.4.1 and § 9.4.2 we resort to the neural influences on cardiovascular variability. Let us recall that:

Physiologically, the origin of the complex dynamics of heart rate has been attributed to antagonistic activity of the two branches of the autonomic nervous system, i.e., the parasympathetic and the sympathetic nervous systems, respectively, decreasing and increasing heart rate [47, 29, 20, 2]. Their net result is what seems to be actually captured by ΔS_l, as shown in § 3.5.3.

A variety of research has now established [35], as already mentioned in § 9.1.3.1, two clear frequency bands in heart rate and blood pressure with autonomic involvement. (i) A higher frequency (HF) band, which lies in [6, 49] the range 0.15 to 0.40 Hz and is [29] "indicative of the presence of respiratory modulation of the heart rate" or reflects [6] "modulation of vagal activity, primarily by breathing". (ii) A lower frequency (LF) band from 0.04 to 0.15Hz (i.e., at around 0.1 Hz), which is usually described as corresponding to [49] "the process of slow regulation of blood pressure and heart rate" or that [6] "it reflects modulation of sympathetic or parasympathetic activity by baroflex mechanisms" due to [29] "the emergence of a limit cycle caused by the vascular sympathetic delay" (note that its exact explanation, however, is still strongly debated [38]). The aforementioned scale $l = 13$ (see ΔS_{13} in Fig. 9.14(b)) corresponds to the LF band, while the scale $l = 3$ (see N_3 in Fig. 9.15), to the HF band. Thus, the magnitude of ΔS_l, when calculated for length

scales corresponding to the HF and LF bands, quantifies the extent to which the processes: "modulation of vagal activity primarily by breathing" and the "slow regulation of blood pressure and heart rate" are "disorganized", respectively.

An alternative way of understanding intuitively the aforementioned findings is the following. If we consider [67] that S could be thought of as a measure of the "disorder" (in successive intervals) and that the essence of the natural time analysis is built on the variation of the durations of consecutive pulses, we may say the following: when approaching sudden cardiac death, the difference between the "disorder" looking in the (immediate) future, i.e., S, and that in the (immediate) past, i.e., S_-, becomes in SD of profound importance when compared to the corresponding difference under truly healthy conditions.

In summary, the complexity measure N_3, based on the entropy change ΔS_l under time reversal at the scale $l = 3$ heartbeats, identifies the sudden cardiac death risk and distinguishes SD from truly healthy individuals as well as from those with the life-threatening congestive heart failure. Furthermore, the study of ΔS_l at the scale $l = 13$ heartbeats provides an estimate of the occurrence time of the impending VF onset in those classified as SD.

The importance of the aforementioned scale of $l = 13$ heartbeats also emerges from studies on the correlation properties of the magnitude and the sign of the increments in the intervals between successive heartbeats during daytime activity as well as during sleep stages. Interestingly, it was found [24, 19] that the correlation behavior of the heartbeat increments and their signs and magnitudes during daytime activity is similar to the behavior in REM (rapid eye-movement) sleep, but significantly different from the behavior in deep sleep. It has been empirically observed [24, 19] by DFA that the most significant differences between the different sleep stages occur in the following ranges: $8 \leq l \leq 13$ and $11 \leq l \leq 150$ heartbeats for the sign-series and magnitude-series respectively. It is challenging that the scale $l = 13$ is just in the verge of these two important ranges. This coincidence cannot be fortuitous, but might stem from the reasons (LF-band, etc.) discussed above.

9.5 Heart rate variability (HRV) and 1/*f* "noise". A model in natural time that exhibits 1/*f* behavior

9.5.1 The 1/*f* "noise". Background

Among the different features that characterize complex physical systems, the most ubiquitous is the presence of $1/f^a$ noise in fluctuating physical variables [36]. This means that the Fourier power spectrum $S(f)$ of fluctuations scales with frequency f as $S(f) \propto 1/f^a$, as already mentioned in § 1.4.2 (see also § 1.5.1.1). The power law behavior often persists over several orders of magnitude with cutoffs present at both high and low frequencies. Typical values of the exponent a approximately range between 0.8 and 4 (e.g., see Ref. [4] and references therein), but in a loose terminology all these systems are said to exhibit $1/f$

"noise". Such a "noise" is found in a large variety of systems, e.g., condensed matter systems(e.g. Ref. [70]), granular flow [43], DNA sequence [45], ionic current fluctuations in membrane channels [40], the number of stocks traded daily [34], chaotic quantum systems [17, 50, 52, 53], human cognition [13] and coordination [72], burst errors in communication systems [5], electrical measurements [28], the electric noise in carbon nanotubes [10] and in nanoparticle films [27], the SES activities (see § 1.4.3), etc. In some of these systems, the exponent a was reported to be very close to 1, but good quality data supporting such a value exist in a few of them [70]. As an example we refer to the voltage fluctuations when current flows through a resistor [71]. As a second example we recall the case of SES activities discussed in § 1.4.3 in which we concluded that $\alpha \approx 1$. As a third example, we mention the case of heart rate variability to which we now turn.

Various tests of time variation have been applied to heart rate variability to show that in healthy subjects heart rate fluctuations display $1/f$ noise and fractal dynamics with long-range correlations, e.g., see Ref. [47]. These initial studies indicated rich dynamics with differences between normal individuals and patients [15]. In particular, it has been found (see Ref. [19] and references therein) that at scales above $\approx$1 min ($l > 60$ heartbeats) the data during waking hours display long-range power law correlations over two decades with average exponents $\alpha_{wake} \approx 1.05$ for the healthy group and $\alpha_{wake} \approx 1.2$ for congestive heart failure patients. These values change to a smaller exponent $\alpha_{sleep} \approx 0.85$ for the healthy group and $\alpha_{sleep} \approx 0.95$ for the heart failure group for the sleep data. Heart rate variability (HRV) is a useful tool that might provide indices of autonomic modulation of the sinus node [58] and its reduced value is a sign of autonomic imbalance. Later findings (e.g., Refs. [21, 18]) showed that healthy heartbeat dynamics exhibits even higher complexity, which is characterized by a broad multifractal spectrum as already mentioned in § 9.2.1 (concerning the distinction between monofractals and multifractals, see § 4.5.1). This high complexity breaks down in illness associated with altered cardiovascular autonomic regulation (e.g., Refs. [29, 19] and references therein). In particular, the heart rate in healthy subjects is a multifractal signal while for subjects with a pathological condition, e.g. congestive heart failure, it shows a clear loss of multifractality [18, 21]. In other words, for the heart failure subjects the multifractal spectrum is nonzero only over a very narrow range of exponents indicating an almost monofractal behavior.

The $1/f^a$ behavior has been well understood on the basis of dynamic scaling observed at *equilibrium* critical points (e.g., § 1.5.3) where the power law correlations in time stem from the infinite-range correlations in space (see Ref. [4] and references therein). Most of the observations mentioned above, however, refer to *non-equilibrium* phenomena for which – despite some challenging theoretical attempts [3, 12] – possible *generic* mechanisms leading to scale-invariant fluctuations have not yet been identified.

In other words, despite its ubiquity, there is no yet universal explanation about the phenomenon of the $1/f^a$ behavior.

9.5.2 An evolution model in natural time that exhibits 1/*f* behavior

We describe here a simple evolutionary model which, in the frame of natural time, leads to $1/f^a$ behavior with an exponent a close to unity.

This model [54] considers the following simple evolution picture. As the number of generations n increases by one, a new species – whose ability to survive is characterized by a number η_n – appears. The new species competes and eliminates *only* the existing species that have a lesser ability to survive. We show below that the number of species ε_n, if considered as a function of the number of generations n, exhibits an $1/f$ behavior and that it increases very slowly with n, actually logarithmically, thus very few species survive in this competitive process.

The mathematical description of the model, in terms of set theory, is as follows. Let us consider the cardinality ε_n (see § 2.7.1) of the family of sets E_n of *successive extrema* obtained from a given probability distribution function (pdf); E_0 equals the empty set. Each E_n is obtained by following the procedure described below for n times. Select a random number η_n from a given pdf (here, we use the exponential pdf, i.e., $p(\eta_n) = \exp(-\eta_n)$) and compare it with all the members of E_{n-1}. In order to construct the set E_n, we *discard* from the set E_{n-1} all its members that are smaller than η_n and furthermore *include* η_n. Thus, $\mathrm{E}_n \neq \emptyset$ for *all* $n > 0$ and E_n is a finite set of real numbers whose members are always larger or equal to η_n. Moreover, $\max[\mathrm{E}_n] \geq \max[\mathrm{E}_{n-1}]$. The increase of the cardinality $\varepsilon_n \equiv |\mathrm{E}_n|$ of these sets is at the most 1, but its decrease may be as large as $\varepsilon_{n-1} - 1$. This reflects an asymmetry if ε_n is considered as time series with respect to the *natural* number n. An example of ε_n vs n is shown in Fig. 9.16(a). The cardinality ε_n exhibits $1/f^a$ noise with a very close to unity; see Fig. 9.16(b). The mathematical model described above, the analytical properties of which has been discussed in detail in Ref. [60], corresponds to an asymptotically non-stationary process, since $\langle \varepsilon_n \rangle \propto \ln n$ with a variance $\langle (\varepsilon_n - \langle \varepsilon_n \rangle)^2 \rangle \propto \ln n$ (see Fig. 9.16(c)). In particular, it has been shown analytically in Ref. [60] that:

$$\langle \varepsilon_n \rangle = \sum_{k=1}^{n} \frac{1}{k}, \tag{9.10}$$

$$\langle (\varepsilon_n - \langle \varepsilon_n \rangle)^2 \rangle = \sum_{k=1}^{n} \left(\frac{1}{k} - \frac{1}{k^2} \right). \tag{9.11}$$

Equations (9.10) and (9.11) reveal that both the average value $\mu \equiv \langle \varepsilon_n \rangle$ and the variance $\sigma^2 \equiv \langle (\varepsilon_n - \langle \varepsilon_n \rangle)^2 \rangle$ diverge logarithmically as n tends to infinity. The point probabilities $p(\varepsilon_n = m)$, however, remain localized around $\mu = \langle \varepsilon_n \rangle \propto \ln n$ since $\sigma/\mu \propto 1/\sqrt{\ln n}$.

Thus, in short, the model suggests that the cardinality ε_n of the family of sets E_n of successive extrema exhibits a logarithmic creep and the $1/f^a$ behavior when considered as time series with respect to the natural (time) number n.

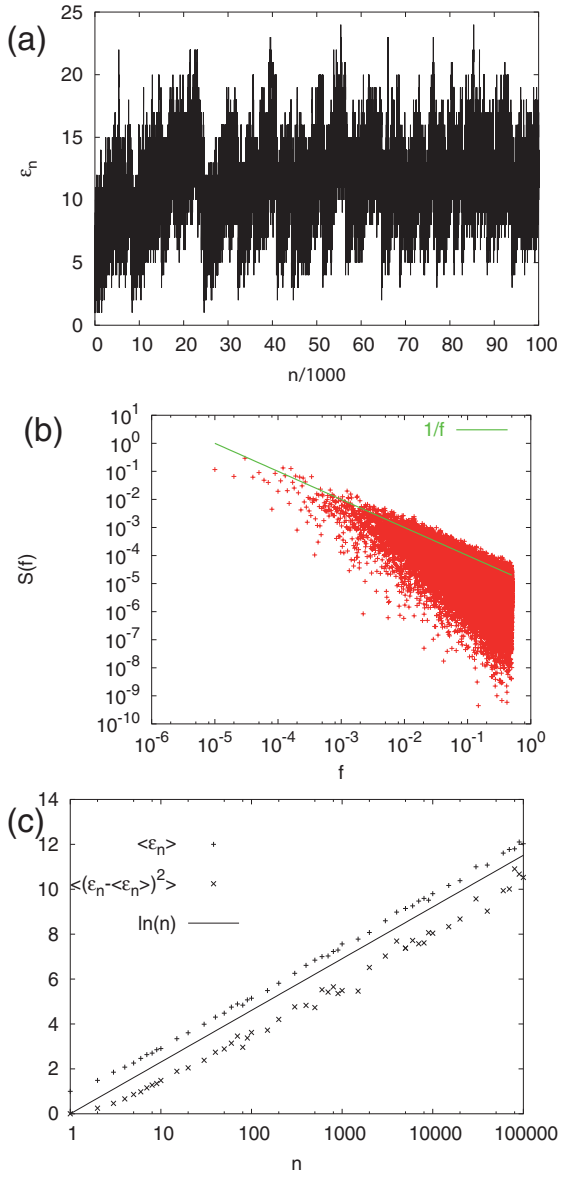

Fig. 9.16 (a): Example of the evolution of ε_n versus the number of generations n, i.e., in natural time. An exponential pdf has been considered for the selection of η_n. (b): The Fourier power spectrum of (a); the (green) solid line corresponds to $1/f$ and was drawn as a guide to the eye. (c): Properties of the distribution of ε_n. The average value $\langle \varepsilon_n \rangle$ (plus) and the variance $\langle (\varepsilon_n - \langle \varepsilon_n \rangle)^2 \rangle$ (crosses) as a function of n. The straight solid line depicts $\ln(n)$ and was drawn for the reader's convenience. Taken from Ref. [54].

Note that an interconnection between $1/f^a$ noise and extreme value statistics has been proposed as providing a new angle at the generic aspect of the phenomena [3].

In order to check the stability of the results of Fig. 9.16, we present in Fig. 9.17(a) the average power spectrum obtained from 10^4 runs of the model. A sharp $1/f$ behavior is observed. Moreover, in Fig. 9.17(b), we present the results of the corresponding average values of F_{DFA-l} of the DFA obtained for various orders l, i.e., when detrending with a

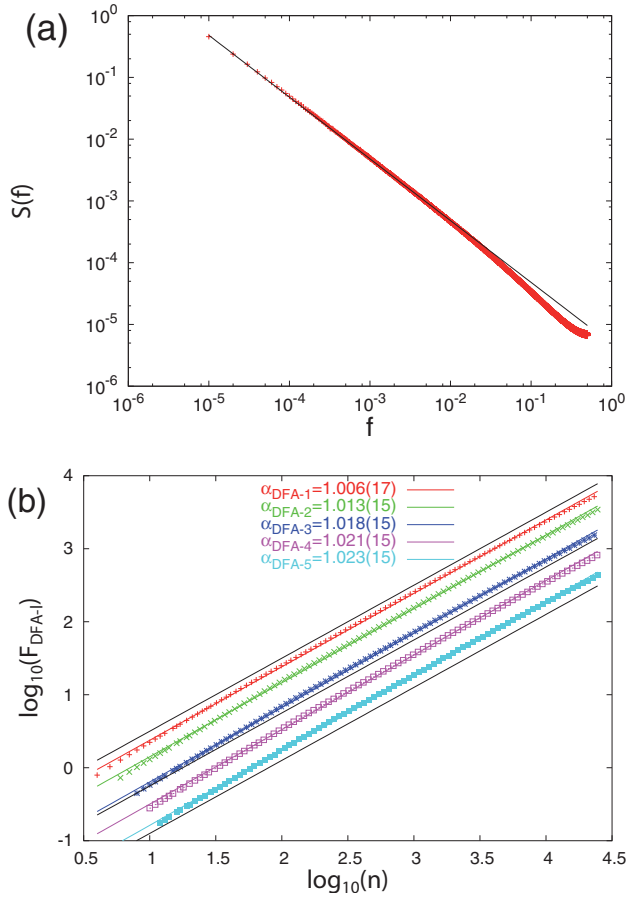

Fig. 9.17 Results from 10^4 runs of the model presented in Fig. 9.16: (a) the average power spectrum, (b) detrended fluctuation analyses of order l (DFA-l). The black solid line in (a) corresponds to $1/f$ spectrum and was drawn as a guide to the eye. For the same reason in (b), the black solid lines correspond to $\alpha_{DFA} = 1$. In (b), the colored solid lines correspond to the least squares fit of the average F_{DFA-l} depicted by symbols of the same color. The numbers in parentheses denote the standard deviation of α_{DFA-l} obtained from the 10^4 runs of the model. The various F_{DFA-l} have been displaced vertically for the sake of clarity. Taken from Ref. [54].

polynomial of order l, see § 1.4.2. Figure 9.17(b) indicates that α_{DFA-l} is close to unity, thus being compatible with the $1/f$ power spectrum depicted in Figs. 9.16(b) and 9.17(a).

We recall that in the aforementioned example of Fig. 9.16(a) showing the evolution of ε_n versus the number of generations n (i.e., in natural time), an exponential pdf has been considered. After investigating several different distributions of η_n, we conclude that the resulting spectral density depends only very weakly – if at all – on the pdf of η_n.

We find that, in order to obtain $\alpha \approx 1$, the only essential condition to be fulfilled is that the corresponding pdf should be bounded from below (note that this is a reasonable assumption if η_n is to be considered a measure of the ability to survive; a negative measure would correspond to a species that is unable to survive).

This holds, of course, under the assumption that η_n come from the *same* pdf, i.e., they are independent and identically distributed variables. Let us now investigate the case when

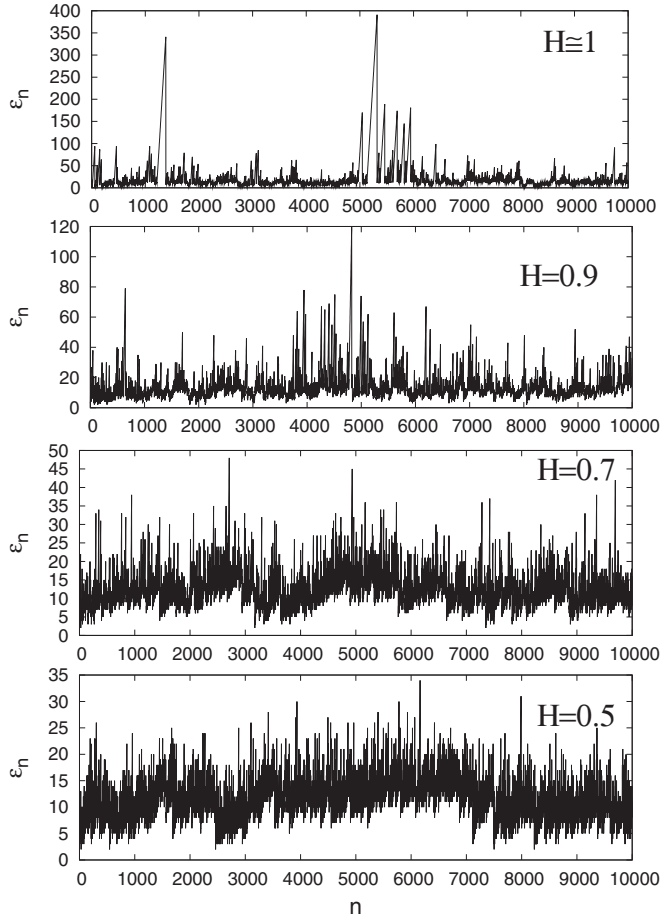

Fig. 9.18 Time series of ε_n when η_n come from fGn for various values of H (increasing from the bottom to the top). Taken from Ref. [54].

η_n come from a stationary but long-range (time) correlated process, for example from fractional Gaussian noise (fGn) (see § 1.5.1.1). To this end, several values of the H exponent have been considered and indicative results are depicted in Fig. 9.18 for $H = 0.5$, 0.7, 0.9 and $\approx$1. A noticeable difference can be visualized in this figure upon increasing H: for $H = 1$, which corresponds, for example, to the case of SES activities (see § 1.4.3, § 4.3.2, § 4.4.2 and Section 4.10) the results differ greatly from those corresponding to smaller exponents, e.g., $H = 0.5$–0.7, which are occasionally found in the analysis of electric signal time series emitted from "artificial" (man-made) electrical sources (see § 4.4.2).

This model, beyond its applicability to HRV (see below in § 9.5.3), may be useful in other disciplines as well. For example, in the frame of a formal similarity between the discrete spectrum of quantum systems and a discrete time series [50], the fol-

lowing striking similarity is noticed. The fact that $a \approx 1$ together with the behavior $\langle(\varepsilon_n - \langle\varepsilon_n\rangle)^2\rangle \propto \ln n$ of the present model, is reminiscent of the power law exponent and the $\langle\delta_n^2\rangle$ statistic in chaotic quantum systems [50, 52].

Furthermore, ε_n may be considered as equivalent to the dimensionality of the thresholds distribution in the so-called coherent noise model (e.g. see Ref. [59] and references therein).

9.5.3 The 1/*f* model proposed and the progressive modification of HRV in healthy children and adolescents

The model described above in § 9.5.2 amounts to a sort of shot noise in a process showing logarithmic creep, a non-stationary process. We now compare this prediction of the model with the heart rate variability data in healthy children and adolescents versus age.

We consider here the HRV data in healthy children and adolescents presented by Silvetti et al. [56]. In particular, the following two standard 24 h time-domain measures, among others, were computed: SDNN (standard deviation of all normal sinus RR intervals over 24 h) and SDANN (standard deviation of the averaged normal sinus RR intervals for all 5-min segments). They evaluated 103 subjects (57 males and 46 females, aged 1–20 years) and found that SDNN and SDANN, overall HRV measures, increased with age and were gender-related. These data demonstrate that in healthy children and adolescents there is a progressive modification of HRV that may reflect a progressive evolution of the autonomic nervous system.

Using the results of Silvetti et al. [56], we plot in Fig. 9.19(a) SDNN vs age in a semilogarithmic plot. An inspection of this figure reveals that, for ages below 14 yr, in both male (blue) and female (red) subjects an almost logarithmic creep is present, a property also exhibited by the model.

This logarithmic creep can also emerge from the results of Ref. [37] where the SDNN versus age (A) was fitted by a power law, i.e., $\mathrm{SDNN} = 97.2 \times \mathrm{A}^{0.20}$ [ms], for the period from infancy to adolescence.

In particular, in Fig. 9.19(b), drawn on the basis of the data presented in fig. 4 of Ref. [37] by using averages every one year of age, a logarithmic creep seems to provide a better description for SDNN from early childhood to adolescence.

This behavior could be, in principle, understood in the following context. The present model may simulate the variation of RR intervals around a mean value determined by the sinoatrial node, thus leading to the logarithmic creep of SDNN visualized in Fig. 9.19. We note that the model intrinsically represents a competitive evolution which is also present

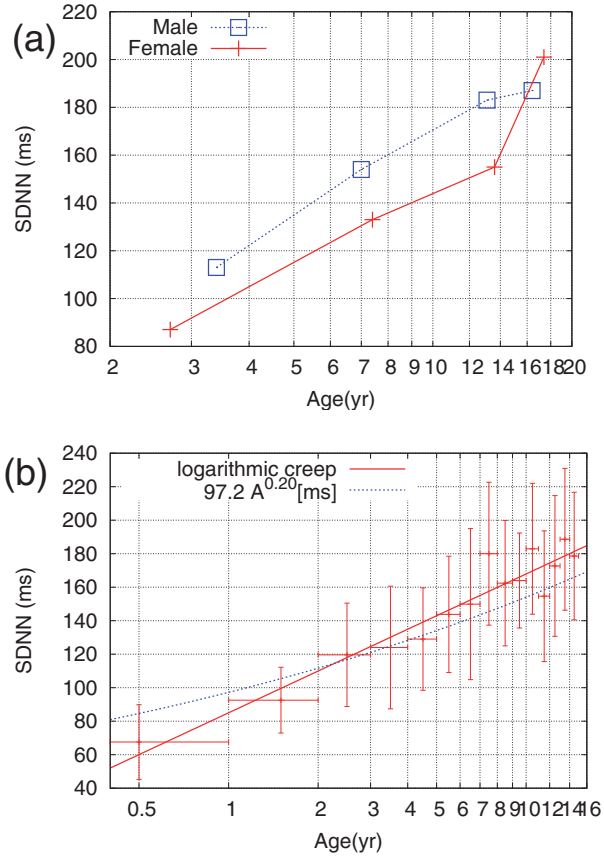

Fig. 9.19 (a): The mean values of SDNN for male (blue) and female (red) subjects as a function of their age. The data come from table 1 of Ref. [56]. The x-axis is in logarithmic scale. (b): Variation of SDNN with respect to age. The data come from fig. 4 of Ref. [37] and are binned every year of age. The vertical error bars stand for $\pm$ one standard deviation. The dotted (blue) curve corresponds to the power law fit suggested in Ref. [37] whereas the solid (red) line corresponds to a logarithmic creep predicted by the model of § 9.5.2. Taken from Ref. [54].

during the period of childhood. The complexity of heart rate dynamics is high in children and illustrates [37]: "an increase of cholinergic and a decrease of adrenergic modulation of heart rate variability with age, confirming the progressive maturation of the autonomic nervous system." In other words, in order to shed light on the underlying connection between the presented model and the development of heartbeat regulation we could say the following. As already mentioned in § 9.4.3, the origin of the complex dynamics of heart rate has been attributed to the *antagonistic* activity of the parasympathetic and sympathetic nervous system:

> It is this *antagonistic* activity which seems to be captured by the model since its basic spirit stems from a competitive evolution process.

9.5.4 The complexity measures obtained from the 1/*f* model and their comparison with HRV data

We now compare the results of the model in natural time with the HRV data – actually the RR time series – of heart disease patients and healthy subjects that have been already analyzed in natural time in Section 9.4. Recall that those data came from long time ECG recordings [14] containing on average $N \simeq 10^5$ heartbeats for each record. Thus, in order to compare with the results already presented in Fig. 9.15(b) on HRV, we consider only mature models with $n \simeq 10^6$ and examine their evolution, i.e, the time series ε_n, for the later 10^5 generations (cf. this is the order of magnitude of heartbeats in a 24 h ECG recording). The proposed model results in $N_3 = 2.52 \pm 0.19$ and $\sigma[\Delta S_7] = (2.46 \pm 0.25) \times 10^{-3}$ shown by the (black) square in Fig. 9.20. This figure just reproduces Fig. 9.15(b) to which the calculated values of the model (as well as those from the INAGS model, see below) are now added. Concerning the calculated value of N_3, this is close to (but below) the minimum value H_{min} observed in H and larger than the N_3 values in the vast majority of SD (where high complexity breaks down). As for the calculated $\sigma[\Delta S_7]$ value, it lies to the right of the maximum value of $\sigma[\Delta S_7]$ observed in H as well as in the vast majority of CHF located outside the shaded region which seems to separate AF from the others. This is consistent with the fact that the (black) square corresponds to an $1/f$ behavior, while healthy heartbeat dynamics exhibits even higher complexity [21, 18] as mentioned in § 9.5.1.

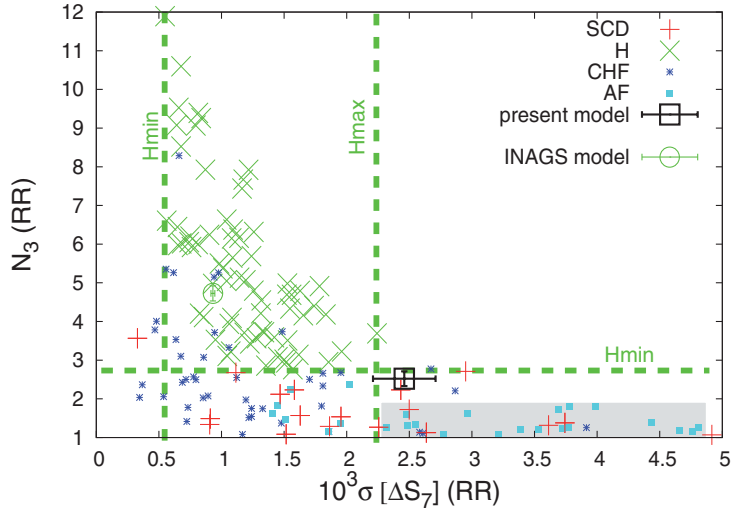

Fig. 9.20 The complexity measure N_3 vs $\sigma[\Delta S_7]$ for the RR time series. This figure is the same as Fig. 9.15(b) to which the complexity measures obtained from the present $1/f$ model as well as those deduced from the model of Ref. [20] have been added, marked with (black) square and (green) circle, respectively. Taken from Ref. [54].

Indeed, let us consider the stochastic feedback model proposed by Ivanov, Nunes Amaral, Goldberger and Stanley (INAGS) in Ref. [20] which describes the *healthy* regulation of biological rhythms with a clear relation to the physiology of the heart; the effects of the sinoatrial node along with the parasympathetic and the sympathetic influences were taken into account. The INAGS model leads [20] to an approximately $1/f^{1.1}$ behavior and generates complex dynamics that account for the functional form and scaling of the distribution of variations of RR. The aforementioned complexity measures in natural time that correspond to this model (by using the same parameters as those mentioned in fig. 2 of Ref. [20]) have been calculated [54] and the results are depicted by the (green) circle in Fig. 9.20. Interestingly, this point lies within the *H-limits*, as it should.

Summarizing, using the concept of natural time, a simple competitive evolution model has been proposed that exhibits $1/f^{a}$ behavior with a close to unity. The model amounts to a sort of shot noise in a process showing logarithmic creep (non-stationary process), a behavior which is similar to the fact that the standard deviation of all normal sinus RR intervals over 24 h exhibits a logarithmic creep with age for children and adolescents. The model predicts complexity measures (see the black square in Fig. 9.20) that separate healthy dynamics from heart disease patients and SD, as intuitively expected since it corresponds to a simple $1/f$ behavior.

References

1. Allexandre, D., Otani, N.F.: Preventing alternans-induced spiral wave breakup in cardiac tissue: An ion-channel-based approach. Phys. Rev. E **70**, 061903 (2004)
2. Amaral, L.A.N., Ivanov, P.C., Aoyagi, N., Hidaka, I., Tomono, T., Goldberger, A.L., Stanley, H.E., Yamamoto, Y.: Behavioral-independent features of complex heartbeat dynamics. Phys. Rev. Lett. **86**, 6026–6029 (2001)
3. Antal, T., Droz, M., Györgyi, G., Rácz, Z.: 1/f noise and extreme value statistics. Phys. Rev. Lett **87**, 240601 (2001)
4. Antal, T., Droz, M., Györgyi, G., Rácz, Z.: Roughness distributions for $1/f^{\alpha}$ signals. Phys. Rev. E **65**, 046140 (2002)
5. Berger, J.M., Mandelbrot, B.B.: A new model for the clustering of errors on telephone circuits. IBM J. Res. Dev. **7**, 224–236 (1963)
6. Bigger J. Thomas, J., Fleiss, J.L., Steinman, R.C., Rolnitzky, L.M., Schneider, W.J., Stein, P.K.: RR variability in healthy, middle-aged persons compared with patients with chronic coronary heart disease or recent acute myocardial infarction. Circulation **91**, 1936–1943 (1995)
7. Bray, M.A.P.: Visualization and analysis of electrodynamic behavior during cardiac arrhythmias. Med. Phys. **30**, 3045 (2003)
8. Chang, T., Sauer, T., Schiff, S.J.: Tests for nonlinearity in short stationary time-series. CHAOS **5**, 118–126 (1995)
9. Chialvo, D.R.: Physiology – unhealthy surprises. Nature **419**, 263 (2002)
10. Collins, P.G., Fuhrer, M.S., Zettl, A.: 1/f noise in carbon nanotubes. Appl. Phys. Lett. **76**, 894–896 (2000)
11. Costa, M., Goldberger, A.L., Peng, C.K.: Multiscale entropy analysis of complex physiologic time series. Phys. Rev. Lett. **89**, 068102 (2002)
12. Davidsen, J., Schuster, H.G.: Simple model for $1/f^{\alpha}$ noise. Phys. Rev. E **65**, 026120 (2002)

13. Gilder, D.L., Thornton, T., Mallon, M.W.: 1/f noise in human cognition. Science **267**, 1837–1839 (1995)
14. Goldberger, A.L., Amaral, L.A.N., Glass, L., Hausdorff, J.M., Ivanov, P.C., Mark, R.G., Mictus, J.E., Moody, G.B., Peng, C.K., Stanley, H.E.: Physiobank, physiotoolkit, and physionet – components of a new research resource for complex physiologic signals. Circulation **101**, E215 (see also www.physionet.org) (2000)
15. Goldberger, A.L., Amaral, L.A.N., Hausdorff, J.M., Ivanov, P.C., Peng, C.K., Stanley, H.E.: Fractal dynamics in physiology: Alterations with disease and aging. Proc. Natl. Acad. Sci. USA **99**, 2466–2472 (2002)
16. Goldberger, A.L., Amaral, L.A.N., Hausdorff, J.M., Ivanov, P.C., Peng, C.K., Stanley, H.E.: Self-organized complexity in the physical, biological, and social sciences: Fractal dynamics in physiology: Alterations with disease and aging. Proc. Natl. Acad. Sci. USA **99**, 2466–2472 (2002)
17. Gómez, J.M.G., Relaño, A., Retamosa, J., Faleiro, E., Salasnich, L., Vraničar, M., Robnik, M.: $1/f^{\alpha}$ noise in spectral fluctuations of quantum systems. Phys. Rev. Lett **94**, 084101 (2005)
18. Ivanov, P.C., Amaral, L.A.N., Goldberger, A.L., Halvin, S., Rosenblum, M.G., Stanley, H.E., Struzik, Z.R.: From 1/f noise to multifractal cascades in heartbeat dynamics. CHAOS **11**, 641–652 (2001)
19. Ivanov, P.C., Chen, Z., Hu, K., Stanley, H.E.: Multiscale aspects of cardiac control. Physica A **344**, 685–704 (2004)
20. Ivanov, P.C., Nunes Amaral, L.A., Goldberger, A.L., Stanley, H.E.: Stochastic feedback and the regulation of biological rhythms. Europhys. Lett. **43**, 363–368 (1998)
21. Ivanov, P.C., Rosenblum, M.G., Peng, C.K., Mietus, J., Havlin, S., Stanley, H.E., Goldberger, A.L.: Multifractality in human heartbeat dynamics. Nature **399**, 461–465 (1999)
22. Jané, R., Blasi, A., J. Garcia, J., Laguna, P.: Evaluation of an automatic threshold based detector of waveform limits in Holter ECG with the QT database. In: Computers in Cardiology, Vol. 24, p. 295. IEEE Computer Society Press, Piscataway, NJ (1997)
23. Kantelhardt, J., Zschiegner, S.A., Koscienly-Bunde, E., Bunde, A., Havlin, S., Stanley, H.E.: Multifractal detrended fluctuation analysis of nonstationary time series. Physica A **316**, 87–114 (2002)
24. Kantelhardt, J.W., Ashkenazy, Y., Ivanov, P.C., Bunde, A., Havlin, S., Penzel, T., Peter, J.H., Stanley, H.E.: Characterization of sleep stages by correlations in the magnitude and sign of heartbeat increments. Phys. Rev. E **65**, 051908 (2002)
25. Kaplan, D., Staffin, P.: (2004). Computer codes `Software for Heart Rate Variability` available from http://www.macalester.edu/∼kaplan/hrv/doc/
26. Khan, I.A.: Long QT syndrome: Diagnosis and management. Am. Heart J. **143**, 7–14 (2002)
27. Kiss, L.B., Klein, U., Muirhead, C.M., Smithyman, J., Gingl, Z.: Diffusive fluctuations, long-time and short-time cross-correlations in the motion of vortice-pancakes in different layers of YBCO/PBCO superlattices. Solid State Commun. **101**, 51–56 (1997)
28. Kogan, S.: Electronic Noise and Fluctuations in Solids. Cambridge Univrsity Press, Cambridge (1996)
29. Kotani, K., Struzik, Z.R., Takamasu, K., Stanley, H.E., Yamamoto, Y.: Model for complex heart rate dynamics in health and diseases. Phys. Rev. E **72**, 041904 (2005)
30. Laguna, P., Jané, R., Caminal, P.: Automatic detection of wave boundaries in multilead ECG signals: Validation with the CSE database. Computers and Biomedical Research **27**, 45–60 (1994)
31. Laguna, P., Mark, R.G., Goldberger, A., Moody, G.B.: A database for evaluation of algorithms for measurement of QT and other waveform intervals in the ECG. In: Computers in Cardiology, Vol. 24, p. 673. IEEE Computer Society Press, Piscataway, NJ (1997)
32. Laguna, P., Thakor, N.V., Caminal, P., Jané, R., Yoon, H.R.: New algorithm for QT interval-analysis in 24-hour Holter ECG - performance and applications. Medical & Biological Engineering & Computing **28**, 67–73 (1990)
33. Lake, D.K., Moorman, J.R., Hanqing, C.: sampen. Computer code `sampen` available from http://www.physionet.org/physiotools/sampen/ (2004)
34. Lillo, F., Mantegna, R.N.: Variety and volatility in financial markets. Phys. Rev. E **62**, 6126–6134 (2000)
35. Malpas, S.C.: Neural influences on cardiovascular variability: possibilities and pitfalls. Am. J. Physiol. Heart. Circ. Physiol. **282**, H6–H20 (2002)
36. Mandelbrot, B.B.: Multifractals and 1/f Noise. Springer-Verlag, New York (1999)

37. Massin, M., von Bernouth, G.: Normal ranges of heart rate variability during infancy and childhood. Pediatr. Cardiol. **18**, 297–302 (1997)
38. McSharry, P.E., Clifford, G.D., Tarassenko, L., Smith, L.A.: A dynamical model for generating synthetic electrocardiogram signals. IEEE Trans. Biomed. Eng. **550**, 289–294 (2003)
39. Melcher, D.: Statist. Computer code STATIST available from http://www.usf.uos.de/~breiter/tools/statist/index.en.html (2001)
40. Mercik, S., Weron, K., Siwy, Z.: Statistical analysis of ionic current fluctuations in membrane channels. Phys. Rev. E **60**, 7343–7348 (1999)
41. Moody, G.B.: Computer code ann2rr available from http://www.physionet.org/physiotools/wag/ann2rr-1.htm.
42. Motulsky, H.: Intuitive Biostatistics. Oxford University Press, New York (1995)
43. Nakahara, A., Isoda, T.: $1/f^{\alpha}$ density fluctuations at the slugging transition point of granular flows through a pipe. Phys. Rev. E **55**, 4264–4273 (1997)
44. Nikolopoulos, S., Alexandridi, A., Nikolakeas, S., Manis, G.: Experimental analysis of heart rate variability of long-recording electrocardiograms in normal subjects and patients with coronary artery disease and normal left ventricular function. J. Biomed. Informatics **36**, 202–217 (2003)
45. Peng, C.K., Buldyrev, S., Goldberger, A., Havlin, S., Sciortino, F., Simons, M., Stanley, H.E.: Long-range correlations in nucleotide sequences. Nature **356**, 168–170 (1992)
46. Peng, C.K., Havlin, S., Stanley, H.E., Goldberger, A.L.: Quantification of scaling exponents and crossover phenomena in nonstationary heartbeat time series. CHAOS **5**, 82–87 (1995)
47. Peng, C.K., Mietus, J., Hausdorff, J.M., Havlin, S., Stanley, H.E., Goldberger, A.L.: Long-range anticorrelations and non-Gaussian behavior of the heartbeat. Phys. Rev. Lett. **70**, 1343–1346 (1993)
48. Pincus, S.M.: Approximate entropy as a measure of system complexity. Proc. Natl. Acad. Sci. USA **88**, 2297–2301 (1991)
49. Prokhorov, M.D., Ponomarenko, V.I., Gridnev, V.I., Bodrov, M.B., Bespyatov, A.B.: Synchronization between main rhythmic processes in the human cardiovascular system. Phys. Rev. E **68**, 041913 (2003)
50. Relaño, A., Gómez, J.M.G., Molina, R.A., Retamosa, J., Faleiro, E.: Quantum chaos and $1/f$ noise. Phys. Rev. Lett. **89**, 244102 (2002)
51. Richman, J.S., Moorman, J.R.: Physiological time-series analysis using approximate entropy and sample entropy. Am. J. Physiol. Heart Circ. Physiol., **278**, H2039–H2049 (2000)
52. Santhanam, M.S., Bandyopadhyay, J.N.: Spectral fluctuations and 1/f noise in the order-chaos transition regime. Phys. Rev. Lett. **95**, 114101 (2005)
53. Santhanam, M.S., Bandyopadhyay, J.N., Angom, D.: Quantum spectrum as a time series: Fluctuation measures. Phys. Rev. E **73**, 015201(R) (2006)
54. Sarlis, N.V., Skordas, E.S., Varotsos, P.A.: Heart rate variability in natural time and $1/f$ "noise". EPL **87**, 18003 (2009)
55. Schreiber, T., Schmitz, A.: Surrogate time series. Physica D **142**, 346–382 (2000)
56. Silvetti, M.S., Drago, F., Ragonese, P.: Heart rate variability in healthy children and adolescents is partially related to age and gender. Int. J. Cardiol. **81**, 169–174 (2001)
57. Siwy, Z., Mercik, S., Weron, K., Ausloos, M.: Application of dwell-time series in studies of long-range correlation in single channel ion transport: analysis of ion current through a big conductance locust potassium channel. Physica A **297**, 79–96 (2001)
58. Taskforce ESC/NASPE: Heart rate variability, standards of measurement, physiological interpretation, and clinical use. Circulation **93**, 1043–1065 (1996)
59. Tirnakli, U., Abe, S.: Aging in coherent noise models and natural time. Phys. Rev. E **70**, 056120 (2004)
60. Varotsos, P.A., Sarlis, N.V., Skordas, E.S.: Seismic electric signals and $1/f$ "noise" in natural time. arXiv:0711.3766v3 [cond-mat.stat-mech] (1 February 2008)
61. Varotsos, P.A., Sarlis, N.V., Skordas, E.S.: Spatio-temporal complexity aspects on the interrelation between seismic electric signals and seismicity. Practica of Athens Academy **76**, 294–321 (2001)
62. Varotsos, P.A., Sarlis, N.V., Skordas, E.S.: Attempt to distinguish electric signals of a dichotomous nature. Phys. Rev. E **68**, 031106 (2003)

63. Varotsos, P.A., Sarlis, N.V., Skordas, E.S., Lazaridou, M.S.: See (the freely available) EPAPS Document No. E-PLEEE8-71-134501 originally from P.A. Varotsos, N.V. Sarlis, E.S. Skordas and M.S. Lazaridou *Phys. Rev. E* **71**, 011110 (2005). For more information on EPAPS, see http://www.aip.org/pubservs/epaps.html.
64. Varotsos, P.A., Sarlis, N.V., Skordas, E.S., Lazaridou, M.S.: See (the freely available) EPAPS Document No. E-PLEEE8-69-107405 originally from P.A. Varotsos, N.V. Sarlis, E.S. Skordas and M.S. Lazaridou *Phys. Rev. E* **70**, 011106 (2004). For more information on EPAPS, see http://www.aip.org/pubservs/epaps.html.
65. Varotsos, P.A., Sarlis, N.V., Skordas, E.S., Lazaridou, M.S.: See (the freely available) EPAPS Document No. E-APPLAB-91-062732 originally from P.A. Varotsos, N.V. Sarlis, E.S. Skordas, and M.S. Lazaridou, *Appl. Phys. Lett.* **91**, 064106 (2007). For more information on EPAPS, see http://www.aip.org/pubservs/epaps.html.
66. Varotsos, P.A., Sarlis, N.V., Skordas, E.S., Lazaridou, M.S.: The use of the entropy in the natural time-domain to distinguish electric signals. Practica of Athens Academy **78**, 281–298 (2003)
67. Varotsos, P.A., Sarlis, N.V., Skordas, E.S., Lazaridou, M.S.: Entropy in natural time domain. Phys. Rev. E **70**, 011106 (2004)
68. Varotsos, P.A., Sarlis, N.V., Skordas, E.S., Lazaridou, M.S.: Natural entropy fluctuations discriminate similar-looking electric signals emitted from systems of different dynamics. Phys. Rev. E **71**, 011110 (2005)
69. Varotsos, P.A., Sarlis, N.V., Skordas, E.S., Lazaridou, M.S.: Identifying sudden cardiac death risk and specifying its occurrence time by analyzing electrocardiograms in natural time. Appl. Phys. Lett. **91**, 064106 (2007)
70. Weissman, M.B.: 1/f noise and other slow, nonexponential kinetics in condensed matter. Rev. Mod. Phys. **60**, 537–571 (1988)
71. Yakimov, A.V., Hooge, F.N.: A simple test of the Gaussian character of noise. Physica B **291**, 97–104 (2000)
72. Yoshinaga, H., Miyazima, S., Mitake, S.: Fluctuation of biological rhythm in finger tapping. Physica A **280**, 582–586 (2000)